

MEASUREMENT AND ANALYSIS OF TEMPORAL VARIATIONS  
OF SALINITY IN SHALLOW WATER

Leonard K Kane

DOLBY DIGITAL LIBRARY  
HAYWARD GRADUATE SCHOOL  
MONTREY, CALIFORNIA 93940

# NAVAL POSTGRADUATE SCHOOL

## Monterey, California



# THESIS

MEASUREMENT AND ANALYSIS OF TEMPORAL  
VARIATIONS OF SALINITY IN SHALLOW WATER

by

Leonard K Kane II

Thesis Advisor:

Noel Boston

Co-Thesis Advisor:

Edward Thornton

Approved for public release; distribution unlimited.

September 1974

7-63100



REPORT DOCUMENTATION PAGE		READ INSTRUCTIONS BEFORE COMPLETING FORM
1. REPORT NUMBER	2. GOVT ACCESSION NO.	3. RECIPIENT'S CATALOG NUMBER
4. TITLE (and Subtitle)  Measurement and Analysis of Temporal Variations of Salinity in Shallow Water		5. TYPE OF REPORT & PERIOD COVERED
7. AUTHOR(s)  Leonard K Kane II		6. PERFORMING ORG. REPORT NUMBER
9. PERFORMING ORGANIZATION NAME AND ADDRESS Naval Postgraduate School Monterey, California, 93940		8. CONTRACT OR GRANT NUMBER(s)
11. CONTROLLING OFFICE NAME AND ADDRESS		10. PROGRAM ELEMENT, PROJECT, TASK AREA & WORK UNIT NUMBERS
12. REPORT DATE September 1974		13. NUMBER OF PAGES 83
14. MONITORING AGENCY NAME & ADDRESS (if different from Controlling Office)		15. SECURITY CLASS. (of this report)  Unclassified
15a. DECLASSIFICATION/DOWNGRADING SCHEDULE		
16. DISTRIBUTION STATEMENT (of this Report)  Approved for public release; distribution unlimited.		
17. DISTRIBUTION STATEMENT (of the abstract entered in Block 20, if different from Report)		
18. SUPPLEMENTARY NOTES		
19. KEY WORDS (Continue on reverse side if necessary and identify by block number)  Salinity, Conductivity, Temperature, Instrumentation, Energy density spectra		
20. ABSTRACT (Continue on reverse side if necessary and identify by block number)  A four electrode conductivity instrument was developed to determine variations of conductivity in an ocean environment at a fixed point. A field experiment was conducted in Mission Bay, San Diego, California. Results indicate that the instrument functioned properly and accurately determined conductivity micro-structure. From conductivity and associated temperature data, salinity data was derived which portrays a well mixed salinity		



## Block 20. (con't)

structure. Difficulty with a mismatch of time constants between conductivity and temperature instruments prevented the accurate determination of salinity microstructure although there was evidence that one existed.





Measurement and Analysis of Temporal Variations  
of Salinity in Shallow Water.

by

Leonard K Kane II  
Lieutenant, United States Navy  
B.S., United States Naval Academy, 1966

Submitted in partial fulfillment of the  
requirements for the degree of

MASTER OF SCIENCE IN OCEANOGRAPHY

from the  
NAVAL POSTGRADUATE SCHOOL  
September 1974

Three  
^  
2

## ABSTRACT

A four electrode conductivity instrument was developed to determine variations of conductivity in an ocean environment at a fixed point. A field experiment was conducted in Mission Bay, San Diego, California. Results indicate that the instrument functioned properly and accurately resolved conductivity microstructure. From conductivity and associated temperature data, salinity data was derived which portrays a well mixed salinity structure. Difficulty with a mismatch of time constants between conductivity and temperature instruments prevented the accurate determination of salinity microstructure although there was evidence that one existed.



## TABLE OF CONTENTS

I.	INTRODUCTION .....	10
II.	CONDUCTIVITY DETECTORS .....	12
A.	CONCEPT .....	12
B.	METHODS OF DETERMINING CONDUCTIVITY .....	13
1.	Two Electrode Conductivity Instrument .....	14
2.	Electrodeless Conductivity Instrument .....	16
3.	Four Electrode Conductivity Instrument .....	18
C.	CONDUCTIVITY INSTRUMENT .....	20
1.	Selection Of Measurement Method .....	20
2.	Construction .....	21
a.	Probe .....	21
b.	Electronics .....	24
III.	LABORATORY AND DOCKSIDE EXPERIMENTS .....	26
A.	LABCRATORY EXPERIMENTS .....	26
B.	DOCKSIDE EXPERIMENT .....	31
IV.	OCEAN SHALLOW WATER EXPERIMENT .....	32
A.	INSTRUMENTATION AND EQUIPMENT .....	32
B.	ARRANGEMENT OF INSTRUMENTS .....	33
C.	EXPERIMENTAL PROCEDURES .....	39
D.	NOTES ON RUNS .....	39
V.	DATA REDUCTION .....	42



VI. DATA ANALYSIS .....	43
A. METHODS OF ANALYSIS .....	43
1. Data Conditioning .....	44
2. Spectral Analysis .....	46
3. Salinity Synthesis .....	47
B. RESULTS OF ANALYSIS .....	47
1. Conductivity And Temperature .....	53
2. Salinity .....	58
VII. CONCLUSIONS .....	77
VIII. BIBLIOGRAPHY .....	78
IX. INITIAL DISTRIBUTION LIST .....	81





## LIST OF FIGURES

1. Two electrode conductivity instrument .....	14
2. Electrodeless conductivity instrument .....	17
3. Four electrode conductivity instrument .....	19
4. Effects of orifice on sample resistance .....	19
5. Conductivity probe .....	23
6. Electronics block diagram .....	25
7. Probe cross-section and electrical equivalent .....	28
8. Instrumentation mounted on frame for Run 12 .....	35
9. Schematic of instrument arrangement on NUC Tower .....	36
10. Relative positions of instruments on frame (side view) .....	37
11. Relative arrangement of conductivity probe and associated thermistor .....	38
12. Inverse filter transfer function .....	45
13. Conductivity and temperature spectra, coherence, and phase - Run 10 .....	49
14. Conductivity and temperature spectra, coherence, and phase - Run 11 .....	50
15. Conductivity and temperature spectra, coherence, and phase - Run 12 .....	51
16. Spectra of waves and vertical fluid particle velocity .....	52
17. Log-log plot of conductivity spectrum - Run 12 .....	55
18. Log-log plot of temperature spectrum - Run 12 .....	56
19. Spectra of temperatures separated 5 cm vertically .....	57



20. Salinity and conductivity spectra, coherence, and phase - Run10 .....	60
21. Salinity and conductivity spectra, coherence, and phase - Run12 .....	61
22. Salinity and temperature spectra, coherence, and phase -Run 10 .....	62
23. Salinity and temperature spectra, coherence, and phase -Run 12 .....	63
24. Log-log plot of salinity spectrum - Run 12 .....	64
25. Regression plot of variances of conductivity and temperature - Run 10 .....	65
26. Regression plot of variances of conductivity and temperature - Run 12 .....	66
27. Time plot of salinity - Run 12 (800 seconds) .....	69
28. Time plot of conductivity in equivalent salinity - Run 12 (800 seconds) .....	70
29. Time plot of temperature in equivalent salinity - Run 12 (800 seconds) .....	71
30. Time plot of salinity - Run 12 (64 seconds) .....	72
31. Time plot of conductivity in equivalent salinity - Run 12 (64 seconds) .....	73
32. Time plot of temperature in equivalent salinity - Run 12 (64 seconds) .....	74
33. Time plot of vertical fluid particle velocity - Run 12 (64 seconds) .....	75



## ACKNOWLEDGEMENT

The author would like to thank his first thesis advisor, Dr. Warren Denner, for initiation of the project and for continued guidance.

The author also thanks his second thesis advisors, Dr. Noel E. Boston and Dr. Edward B. Thornton for their assistance and guidance throughout the project.

In addition, the author would like to express his appreciation to Dr. Robert G. Paquette for providing necessary information concerning conductivity instruments and for making helpful comments on this report.

The Office of Naval Research is gratefully acknowledged for the funding without which this project would not have been possible.

Finally, the efforts and ideas of LT James B. Hagen, USN, my classmate and co-worker, were deeply appreciated and significant in the accomplishment of this project.



## I. INTRODUCTION

In recent years the studies of ocean parameters - temperature, salinity, sound velocity - have been extended from the large scale to the small. The increased emphasis on small scale phenomena has been due in large part to improved instrumentation. The use of thermistor beads [Osborn and Cox 1972, Neshyba et.al. 1972, and others] has shown that small scale temperature microstructure exists almost universally in the oceans. Velocity microstructure has been observed with hot-film anemometers [Grant et.al. 1968] and recently electrical conductivity measuring instruments have shown the existence of small scale salinity microstructure [Stommel and Federov 1968].

The temperature and salinity microstructure result in an interesting by-product. Since sound velocity is a function of these parameters it is logical to assume that a sound velocity microstructure also exists. The only certain way of establishing this is to measure all parameters, including sound, in situ in a given volume of seawater and analyze the resulting data to determine statistical relationships between parameters. Such has been one of the objectives of a program carried out in the Department of Oceanography of the U.S. Naval Postgraduate School for the past few years. The study was inaugurated in October 1971 when Seymour [1972], Duchock [1972] and Bordy [1972] first attempted to do this. In June 1972 a second experiment was conducted by Frigge [1973], Gossner [1973] and Whittmore [1973]. Of particular interest to this present study was the work of Frigge who examined the salinity sensing capability of a model 9006 STD and found it unsuitable for sensing salinity microstructure fluctuations. The STD was unsuitable because it had a salinity sensor with too long a temperature compensation time constant for the scales sought and because





reliable measurements of salinity required a continuous flow of water past the sensor. Frigge attempted to operate it at fixed depths where the flow velocity would frequently pass through zero as the water oscillated past the sensor with the waves. Clearly an improved instrument was needed which would have improved frequency response and be velocity independent. Such an instrument would allow one to determine reliable statistical relationships between salinity, temperature and sound velocity.

The intention of this study was to develop, test and try such an instrument in a real ocean environment. The secondary objective was to provide data for determining statistical relationships between the aforementioned parameters should the instrument prove to be successful.



## II. CONDUCTIVITY DETECTORS

### A. CONCEPT

The measurement of salinity is normally accomplished by one of two methods. The first is the traditional method of chemically determining the chlorinity of a seawater sample. The salinity can then be obtained by the empirical relationship formulated by an International Commission in 1902 composed of C. Forch, M. Knudsen and S.P.L. Sorensen. Their equation was later modified by research conducted by R.A. Cox, F. Culkin and J.P. Riley. In 1966, The National Institute of Oceanography of Great Britain and UNESCO jointly published the results of this research as The International Oceanographic Tables. These tables contain the presently used new definition of salinity which is:

$$S\% = 1.80655 \text{ Cl}\% \quad (1)$$

The other method now in wide use to determine the salinity of seawater depends on the property of the electrical conductivity of a seawater sample. Electrical conductivity is primarily a function of the salinity and temperature of the sample. Empirically, salinity has been defined as the ratio of the conductivity of the sample to the conductivity of a standard seawater sample. The standard seawater has a salinity of exactly 35‰. The standard conditions for determining the ratio are a sample temperature,  $T$ , of 15°C at a pressure of one atmosphere. Sample salinity is then given by:



$$S\text{‰} = -0.08996 + 28.2972 R_{15} + 12.80832 R_{15}^2 - 10.67869 R_{15}^3 + 5.98624 R_{15}^4 - 1.32311 R_{15}^5 \quad (2)$$

where

$R_{15}$  = conductivity ratio at 15°C

This empirical equation was also published in the International Oceanographic Tables in 1966 as a result of the research by Cox , Culkin and Riley.

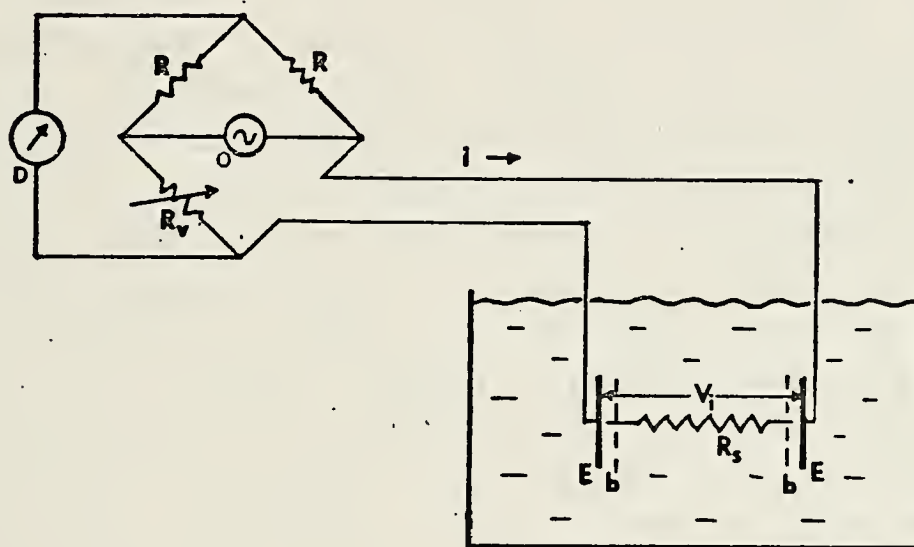
#### B. METHODS OF DETERMINING CONDUCTIVITY

Electrical conductivity of a seawater sample is normally measured in one of three ways. In each case, as variations of temperature, salinity and possibly flow occur, there is a corresponding variation in the sample conductivity. Conductivity is directly related to the ion concentration and mobility in the sample. As salinity increases, more ions are available and the sample conductance will increase. As the temperature of the sample increases, the ions are more mobile and sample conductance increases. Flow affects conductance if a high power level is used by the sensor. As the power is dissipated within the sample, there is an increase in sample temperature which in turn causes an increase in conductivity. Sample flow past the sensor removes the heat. The higher the flow rate, the less will be the effect of power dissipation on conductivity. The variations in conductivity due to salinity, temperature and flow variations may be quite small, but with sensitive electronic equipment, they may be accurately measured.



## 1. Two Electrode Conductivity Instrument

The oldest and simplest method to measure conductivity of a seawater sample uses two fixed electrodes. These electrodes are immersed in the sample and serve to carry a constant current through the sample. This current develops a voltage potential between the electrodes proportional to the sample's electrical resistance in accordance with Ohm's Law. This voltage potential is sensed by the electrodes and is measurable with an electronic circuit which is usually some form of a Wheatstone bridge (Fig. 1).



- D - Detector
- O - Oscillator
- R - Bridge resistors
- R<sub>v</sub> - Variable resistor
- I - Current
- E - Electrodes
- b - Boundary layer
- R<sub>s</sub> - Sample resistance
- V<sub>i</sub> - Induced voltage

Figure 1. - Two electrode conductivity instrument.





From this bridge, a measured value of sample resistance is obtained and the sample's conductivity can then be determined from the equation:

$$\sigma = 1/hR \quad (3)$$

where

$\sigma$  = sample conductivity

h = calibrated cell constant

R = measured resistance

While this type of conductivity instrument has been widely used in laboratories, it suffers from several problems. The major problem is an effect called electrode polarization. When a direct current is applied across two electrodes immersed in an electrolyte, electrolysis occurs. The electrolyte in the boundary layer then changes composition and a galvanic potential develops at the electrode interface. This results in an increased resistance in the boundary layer which may be a substantial percentage of the actual resistance of the electrolyte. The measured resistance of the sample as determined by the observed voltage potential will then be in error. To reduce this polarization effect a sinusoidal current is applied instead of a direct current. This causes a periodic fluctuation of the boundary layer resistance. The higher the sinusoidal frequency, the smaller the polarization. However the readjustment of the boundary layer does not occur simultaneously with the changes in the current so that there is now a lag in phase between the applied current and the observed developed voltage. A complex impedance results with resistive and capacitive components from which it is difficult to determine the actual sample resistance.

As an interesting sidelight, L.L. Higgins [1962] has shown that if the frequency is increased enough, it is possible to separately determine the actual temperature and salinity using the two electrode conductivity instrument.



To do this both the resistance and the reactance of the measured electrical impedance must be determined. However the frequencies involved, approximately 1 - 5 kHz, are so high that serious problems occur such as large wiring capacitive leakage. To design such an ocean going instrument would be extremely difficult.

Another problem which exists with a two electrode instrument is contributions of stray electrical currents to the measured sample impedance. The stray current will cause an unwanted and unknown voltage between the probes which means a false impedance will be determined. These stray currents are particularly present near ships and structures from which measurements in the ocean may be made.

## 2. Electrodeless Conductivity Instrument

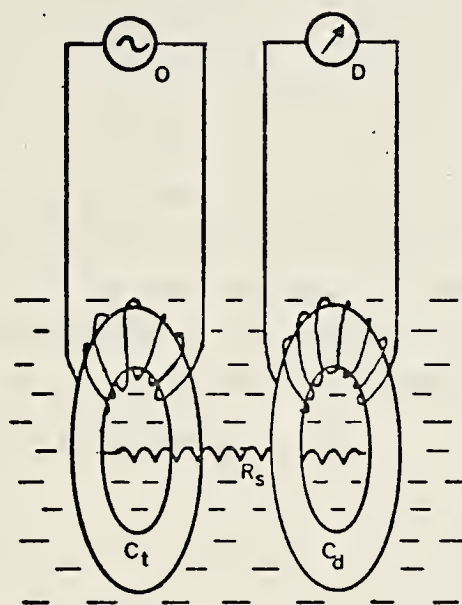
A method which eliminates electrode polarization uses the transformer induction principle to measure sample conductance. In the normal configuration an alternating current is applied to a toroidal coil acting as a current transformer immersed in the sample. A second coil, acting as the detector coil of the current transformer, is linked to the first by the conducting sample. As the sample conductance varies, the voltage output of the second coil varies proportionately (Fig. 2).

This method has been used successfully in standard oceanographic equipment such as the STD and bench salinometers. While the principle of operation of these instruments is simple, construction of the sensor is difficult. J.E. Diamond [1970] discusses the construction of an inductive conductivity meter. To eliminate stray coupling between the coils, the coils must be heavily shielded. This means that the detector is usually large with an outside diameter of 5 to 8 cm and an inside diameter of 2 to 3 cm. Proper design requires a transmitting coil with high voltage per turn, low magnetizing current and low



losses. The detector coil must be current sensitive, have a low input impedance and short heavy leads. This last feature may require a separate preamplifier located near the coil if the detector is placed far from the rest of the electronics.

Another difficulty arises when sensing a varying conductivity with the large induction sensor. A large flushing volume is required to give an accurate representation of the conductivity changes. While not a problem in a sensor which is continuously lowered into the ocean such as the STD is, it can be a problem with measurements at a fixed point.



- O - Oscillator
- D - Detector
- $R_s$  - Sample Resistance
- $C_t$  - Transmitting Coil
- $C_d$  - Detecting Coil

Figure 2. - Electrodeless conductivity instrument.





### 3. Four Electrode Conductivity Instrument

A third way to measure electrical conductivity of a seawater sample is similar to the first. However, to eliminate the effects of electrode polarization on the measurements, four electrodes are used instead of two. One pair, referred to as the driver electrodes, has an alternating current applied to them. The second pair, the sensing electrodes, are located between and away from the polarized boundary layers of the driver electrodes (Fig. 3). The alternating current develops an alternating voltage in the sample which is measured by the sensing electrodes. With a high input impedance in comparison to the sample resistance, little current will flow through the sensing electrodes. With little current flow, there will be no noticeable polarization effect at these electrodes. The measured impedance will thus be the correct impedance of the sample.

A technique which may be used with this type of instrument to increase its sensitivity is to place the sensing electrodes on either side of a small diameter tube filled with the sample to be measured (Fig. 4). This has the effect of increasing the measured resistance in accordance with the equation:

$$R = L / (\pi r^2 \sigma) \quad (4)$$

where

L = length of orifice

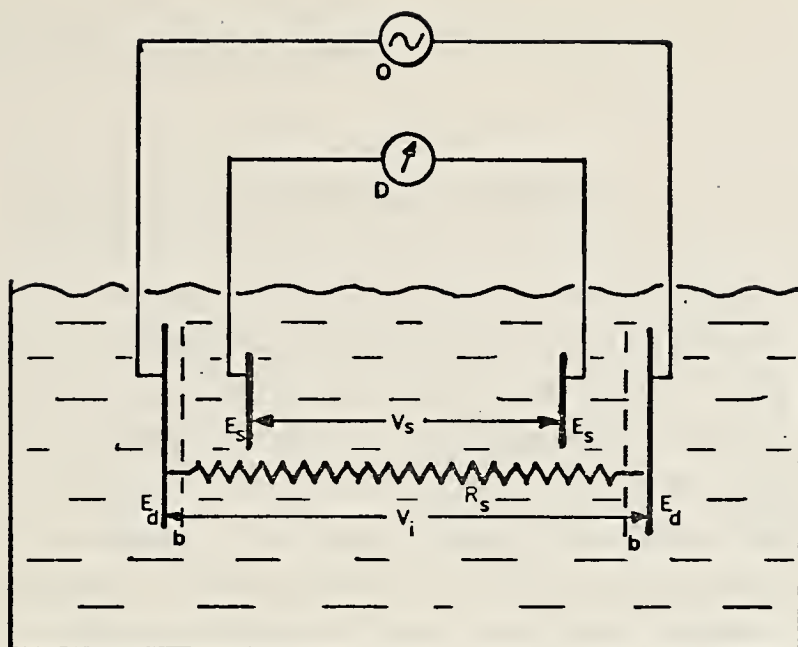
r = radius of orifice

$\sigma$  = conductivity of the fluid

As with the two electrode conductivity instrument, stray currents could still be a problem with this type of instrument.







- $E_d$  - Driving electrodes
- $E_s$  - Sensing electrodes
- $R_s$  - Sample resistance
- $V_i$  - Induced voltage
- $V_s$  - Sensed voltage
- $b$  - Boundary layer
- O - Oscillator
- D - Detector

Figure 3. - Four electrode conductivity instrument.

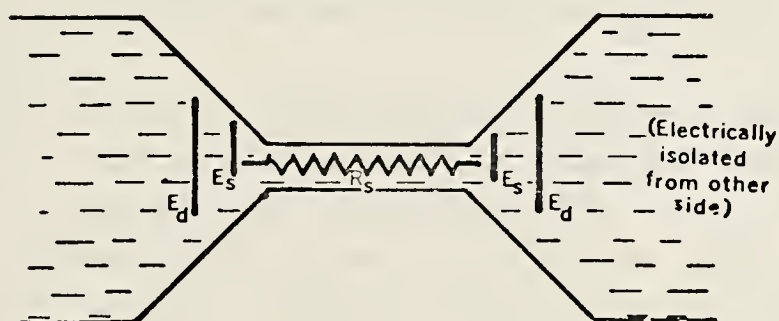


Figure 4. - Effect of orifice on sample resistance.



## C. CONDUCTIVITY INSTRUMENT

### 1. Selection Of Measurement Method

All three methods allow remote continuous sensing of electrical conductivity which can be related to salinity by equation (2). Initially in this research, the induction probe was considered to have the greatest chance of success. However, because of the large size of most available induction sensors, it was felt that they would seriously disturb the very microstructure which they were to measure. Salinity microstructure is on the order of several centimeters [Osborn and Cox 1972] and with a probe of the same or larger magnitude, the microstructure may not even be sensed.

Further, the large inside diameter requires a large flow of water through the coil to provide a time constant consistent with the spatial scales of the salinity microstructure. In the case of Frigge [1973] who tried to use this type of probe at a fixed depth, such flow rates were not available. As a result his comparisons with thermistors, whose time constants were about 0.1 seconds, suffered. The problems of long time constants encountered by Frigge with the STD provided considerable incentive for this present study.

A smaller induction probe may have allowed smaller scale measurements. However, none were available for this study. Additional investigation also indicated that they still required a larger flow rate through the coil than was permissible for the study of small salinity scales. These probes are better adapted for measurement of conductivity while moving through the medium than for measurement at a fixed point.



The two electrode conductivity sensor did not appear to be well suited for microstructure measurements. Problems with polarization limit its effectiveness to accurately measure varying salinity.

The development of a four electrode conductivity probe seemed to offer the best solution. Gregg and Cox [1971] had already used such a probe on a free fall vehicle which descended to considerable depths. Discussion with Gregg (December 1973) indicated that it might be possible to modify it for fixed point measurements in shallow water. Subsequently schematics of their electronics package were obtained but only a rough sketch and photograph of the actual conductivity probe were available. With these and conversations with Gregg, a probe was built.

## 2. Construction

The conductivity instrument which was built had to be reliable in order to take continuous measurements over a period of hours. It also needed to be simple and rugged in order to withstand the rough environment of the upper few meters of the ocean.

### a. Probe

The probe consisted of a piece of machined 2.54 cm diameter plexiglass rod (Fig. 5). The only critical dimension was the diameter of the orifice which must be small to increase the measured electrical resistance of the sample flowing through it, but not so small that adverse mechanical heating of the sample occurred. The resistance can be determined by equation (4). For this probe 1.5 mm was chosen as the diameter with a length of about .25 cm.

Cylindrical platinum blacked platinum electrodes were used for both sets of electrodes. The sensing electrodes were located as near as possible to the orifice in order to provide the least amount of signal from volumes other than



the orifice. The driving electrodes, whose location is less critical, were located further away.

Flow through the probe was provided by a vacuum pump connected to the probe by 30 m. of plastic tubing. A large 20 liter reservoir collected the water and served as a filter to dampen any pump induced oscillations in the flow. Flow rate was controlled by a valve in the suction line to maintain approximately 0.5 ml/sec.





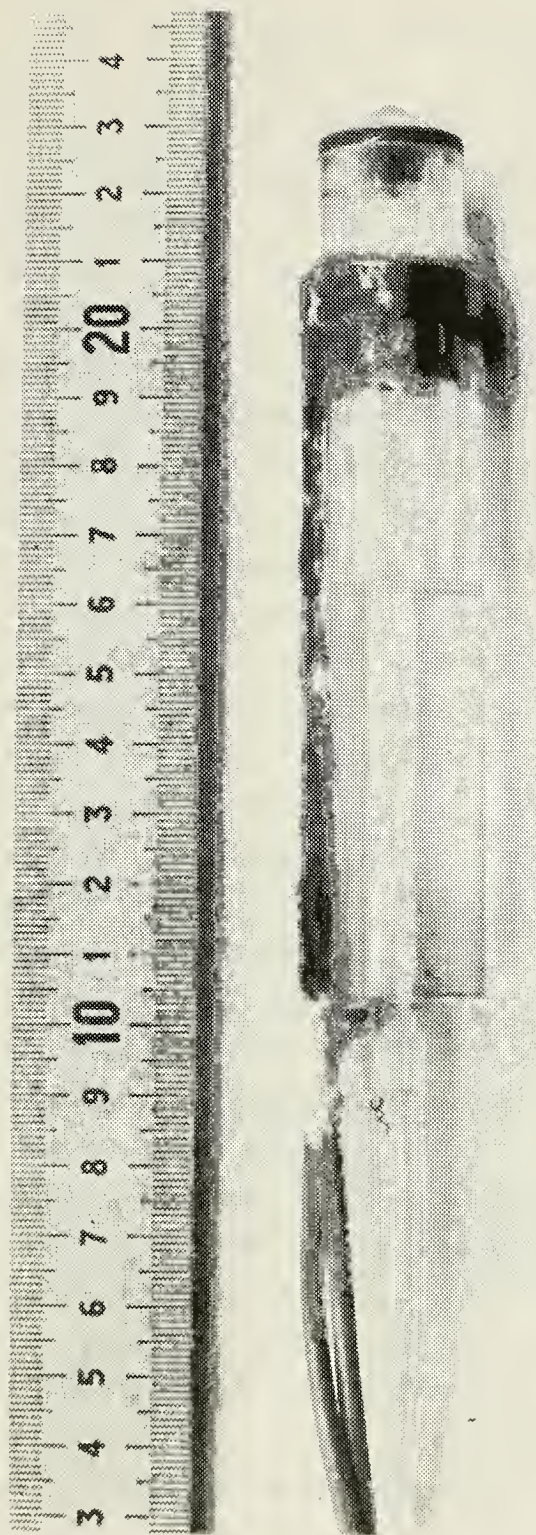


Figure 5. - Conductivity probe.



## b. Electronics

The electronics consisted of a driving section and a sensing section (Fig. 6). A 1 kHz squarewave signal from a signal generator is fed to the driving section where it causes two field effect transistors to fire on positive and negative pulses. This provides a constant 1.35 v amplitude 1 Khz square wave signal to a constant current regulator. The current regulator slightly amplifies the signal dependent on a fixed gain setting and then applies it to the driving electrodes via an isolation transformer. The signal current through the seawater sample causes a voltage to be developed which is inversely proportional to the conductivity of the sample. As the conductance of the seawater flowing through the probe changes, the developed voltage also changes. It is this voltage which is picked up by the sensing electrodes and fed via another isolation transformer to the sensing section.

In the sensing section, the voltage signal, which is still a 1 Khz square wave, is first full-wave rectified and then amplified by a low-noise linear IC amplifier. A bucking signal is also applied to the amplifier to null out the large D.C. level of output which would be several orders of magnitude larger than the variations being measured. From the amplifier the signal is next filtered using an RC filter to remove the remaining 1 KHz carrier signal. The final resultant signal level is inversely proportional to the variations of conductivity sensed by the probe and it is this signal which is analyzed.

For this project a total of three probes and two electronic units were built. The second two probes had slightly smaller but longer orifices to increase the resistance. This provided a larger voltage change for the same change in conductivity, i.e. it made the probes more sensitive.



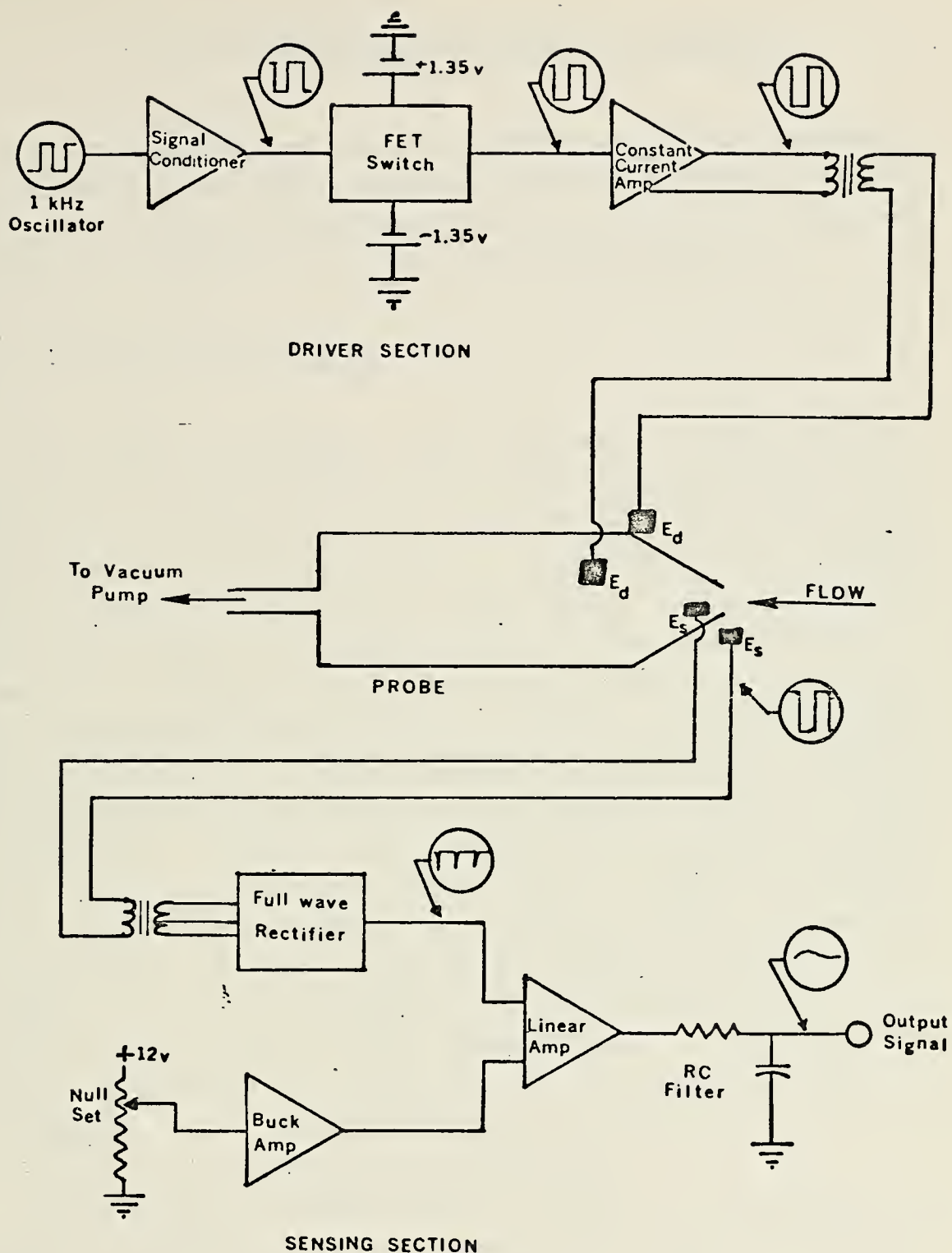


Figure 6. - Functional block diagram of conductivity instrument electronics.





### III. LABORATORY AND DOCKSIDE EXPERIMENTS

After construction of the instruments it was necessary to verify that they did in fact measure variations of salinity. Calibration of the instruments was also necessary in order to determine the size of the variations.

#### A. LABCRATORY EXPERIMENTS

The first experiment was designed to verify that the probe did measure variations of salinity. The probe was placed in a large beaker of seawater and then as a sample was taken through the probe, a 1 ml burette of distilled water was added near the tip of the probe. As the distilled water was added, the voltage output of the instrument, as read on a digital voltmeter, was observed to fluctuate. After completely mixing the new solution, the voltage level was now steady and slightly higher than originally. This was as expected for a now less saline solution having a lower conductivity. During this experiment it was also observed that voltage fluctuations occurred if the probe was brought near the beaker sides or bottom. This was due to interference of the electrical conducting path by the beaker. It did not appear to be a problem as long as the probe remained greater than approximately 1 cm from the beaker. From this experiment it was apparent that the instrument would measure salinity variations but the magnitude still needed to be determined.

The second experiment was an attempt to calibrate the probes. A first attempt was made using a bench salinometer. The sample was drawn into the salinometer through the probe. Voltage readings were taken on the conductivity instrument while sampling and then temperature and salinity were



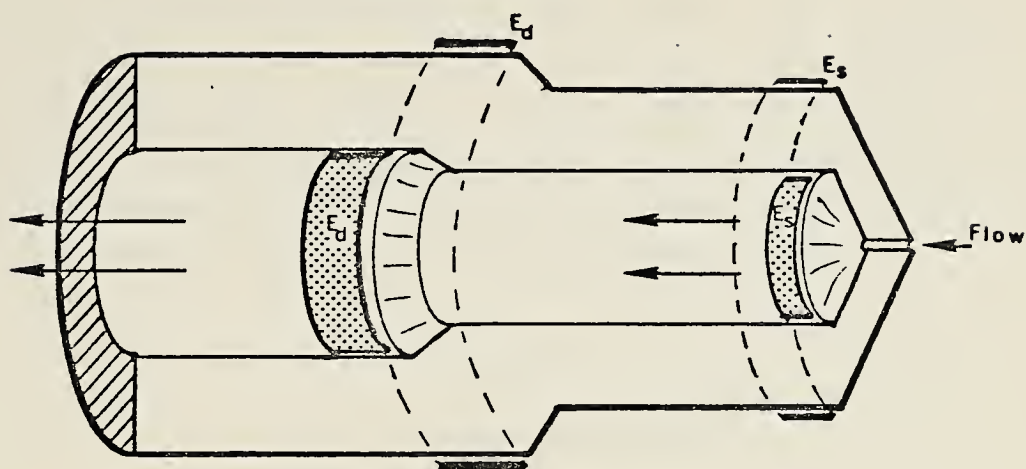


obtained from the salinometer. However while sampling, the instrument voltage fluctuations were very large and erratic. They were also nonrepeatable when taking a second sample. It was decided that this fluctuation was caused by bubble cavitation in the orifice. As the sample was drawn through the orifice, a pressure drop occurred which was enough to allow bubbles to come out of solution and greatly change the effective measured conductivity. While this cavitation prevented calibration of the probes in this manner, it would present no problem in the ocean where the sample would be drawn in at greater pressures which would prevent cavitation.

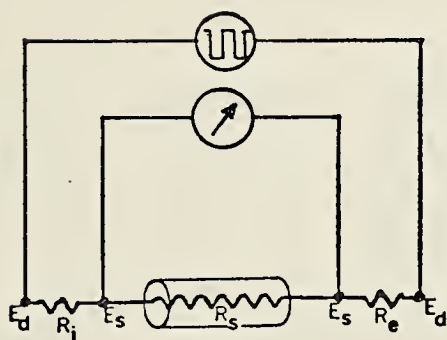
A second method to calibrate the probes proved more fruitful. It was found that a decade resistance box could be substituted for the probe. Later (April 1974) it was learned from Gregg that this was basically the technique he also used to calibrate his instrument. First a sample was obtained through the probe by siphoning in order to prevent cavitation. As the sample was taken, the instrument voltage was nulled to zero. Also at this time the temperature of the solution being sampled was obtained with a quartz thermometer. Once the sample was obtained, the probe was disconnected and the resistance box inserted in its place (Fig. 7). By adjusting the resistance the instrument voltage was brought to zero. The resistance thus obtained was equal to the resistance of the sample as measured by the probe. The actual salinity of the sample was obtained by normal methods using a bench salinometer. Calibration was performed over the range of 20 to 40 ppt.



# CROSS-SECTION



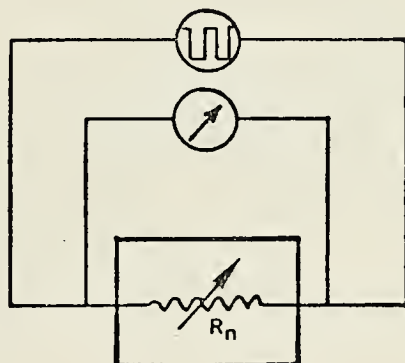
## ELECTRICAL EQUIVALENT



$R_s$  - Sample resistance  
 $R_i$  - Interior resistance  
 $R_e$  - Exterior resistance

$$R_s \gg R_i, R_e$$

a) With probe



$R_n$  - Null resistance

$$R_n = R_s$$

b) With decade box

Figure 7. - Probe cross-section and electrical equivalent.



With this data and nomographs of the resistivity of seawater as a function of salinity and temperature from Higgins [1962], the probes were calibrated. The calibrated cell constants were in reasonable agreement with theoretical values obtained using equations (3) and (4) (Table I). Differences may be accounted for by the inaccuracies of dimensions in the manufacture of the probes, i.e. length and diameter of the orifice not exactly as specified.

TABLE I  
PROBE CHARACTERISTICS

Probe	$h_{\text{theoretical}}$ cm/ohm	$h_{\text{calibrated}}$ cm/ohm	sensitiv %/volt	transient time sec
1	0.028	0.026	.0002	.008
2	0.035	0.041	.0003	.009
3	0.055	0.049	.0004	.007

The calibration factor,  $C$ , for changing instrument voltage output to resistance was determined from the instrument voltage change for an ohm change of the decade box. The factor was found to be 50.48 ohm/volt.

Using these calibration factors, the change in actual resistance of a sample is given by:

$$\Delta r = h \Delta V C \quad (5)$$

where

$\Delta V$  = change in output voltage



Sensitivity of the instrument can then be determined from the following equation [Higgins 1962].

$$B_s \Delta S\% = - \Delta r / r_0 + B_t \Delta T \quad (6)$$

where

$r_0$  = seawater resistance

at temperature  $T_0$

and salinity  $S_0\%$

$B_s$  = salinity coefficient

$$= 1/r_0 [\partial r / \partial S\%]$$

$B_t$  = temperature coefficient

$$= 1/r_0 [\partial r / \partial T]$$

If temperature is assumed constant with  $T_0 = 13^\circ\text{C}$  and  $S_0\% = 33.6\%$  and a voltage sensitivity of 0.01 mv is assumed for the digital voltmeter or data recording system, the sensitivity may be determined as indicated in Table 1. This sensitivity was judged sufficient for the requirements of the experiment to be conducted.

The sensitivity of the instrument to flow rates through the probe was also checked. With no flow the instrument provided a constant voltage reading. But as flow was initiated the voltage changed to a new level which was constant regardless of flow rate in the range of 0.1 to 2.0 ml/sec. If a nominal flowrate of 0.5 ml/sec is chosen, the transient time of a sample through the probe is less than .01 sec.

The frequency response of the instrument can now be determined. The probe output voltage change for a corresponding change in conductivity is for all practical





purposes instantaneous. Hence, frequency response of the instrument is determined by the flow rate through the probe and by the time constants of the electronics. The time constant of the electronics unit is the larger of the linear amplifier and the following RC filter. The linear amplifier has a linear response out to 100 kHz with a time response of 5  $\mu$ sec. The RC filter has a time constant of 3 msec. From this it can be seen that the limiting response time of the instrument is that of the flow rate, a nominal 8 msec. This implies a frequency response for the instrument of about 0 to 100 Hz.

With this type of response, it was not felt necessary to determine the length constants of the probes. (Length constant is the relative distance through which the probe must move to give a 63% change in response to a change in conductivity.)

#### B. DOCKSIDE EXPERIMENT

A dockside experiment was conducted off the Coast Guard pier in Monterey Bay to determine if the entire system would function properly. Data was recorded on a strip chart recorder. Two probes were used simultaneously. Everything appeared to work well. Periodic fluctuations were observed in the records of both probes and thought due to wave motion on the temperature structure. As the probes were moved up and down large changes in the voltages were observed which probably corresponded to temperature changes with depth. As no thermistors were used in conjunction with the probes, this was not verified. With calibration and preliminary testing completed, the instruments were thought ready for trial in the ocean.



#### IV. OCEAN SHALLOW WATER EXPERIMENT

The real trial for these conductivity probes was conducted off the Naval Undersea Center's offshore tower, near San Diego, California. This tower is located about one mile offshore in Mission Bay in 19 meters of water. The experiment was designed to measure the in situ parameters of sound amplitude and phase, temperatures, conductivity, wave height, and fluid particle velocity within a relatively small volume of seawater (3 m X 3.5 m X 2 m).

##### A. INSTRUMENTATION AND EQUIPMENT

The following instruments were used for this experiment.

###### 1. Conductivity Sensors (2)

Time constant	8 msec
Salinity range	20-40 ppt
Sensitivity	$\pm 0.0004$ %/volt

###### 2. Thermistors (14)

Time constant	150 msec
Temperature range	10-16 °C
Accuracy	$\pm 0.006$ °C

A detailed description is given by Hagen [1974].

###### 3. Baylor Wave Height Sensor

Accuracy	$\pm 1\%$ of reading
----------	----------------------

A detailed description is given by Krapohl [1972].

###### 4. Water Particle Velocity Sensor (3)

A detailed description is given by Bub [1974].



## 5. Sound Transducer

USRD Model F-33

A detailed description is given by Hagen [1974].

## 6. Sound Hydrophones (3)

USRD Model F-50

A detailed description is given by Hagen [1974].

A total of 28 instrument outputs were recorded on a Sangamo Magnetic Tape Resorder Model 3562 and a Sabre III Magnetic Tape Recorder. Each had 14 channels and was operated at 3 3/4 ips. Channel allocation was made to record 12 of the 14 thermistors on the Sabre III recorder. The other two channels were used to record conductivity in order to record them on the same tape as their adjacent thermistors to which they were attached. The other two thermistors and the remaining instrument signals were recorded on the Sangamo recorder.

## B. ARRANGEMENT OF INSTRUMENTS

The instruments were arranged on a 2 inch pipe frame mounted on a trolley on the seaward (west) side of the tower. The trolley with the frame could then be lowered to any depth above the ocean floor (Figs. 8 and 9).

The thermistors were arranged in a vertical plane along the right side of the frame. Seven thermistors were placed in a vertical row and eight thermistors were in a horizontal row with one thermistor in common between the rows (Fig. 10).

Each conductivity probe was mounted in a horizontal position directly onto a thermistor probe so that there existed a 4 cm separation between the thermistor and the



conductivity probe tip (Fig. 11). This close spacing was necessary so that salinity changes could be computed from equation (6). For runs 1 through 8, this was a horizontal separation and for runs 9 through 12, a vertical separation. Probe No. 1 was mounted on the horizontal thermistor row and probe No. 2 was mounted at the intersection of the rows.

The sound array was mounted on a rotatable arm in the center of the frame. The centerline of the array was 57 cm from the thermistor array plane with the sound array horizontal for runs 1 through 9. For run 10 the array was vertical and for runs 11 and 12 it was at a  $25^\circ$  angle to the vertical. The particle velocity sensors were placed in three locations in a vertical row in line with and almost in the same plane as the vertical thermistors.

The Baylor wave gage was mounted directly above the vertical thermistors.





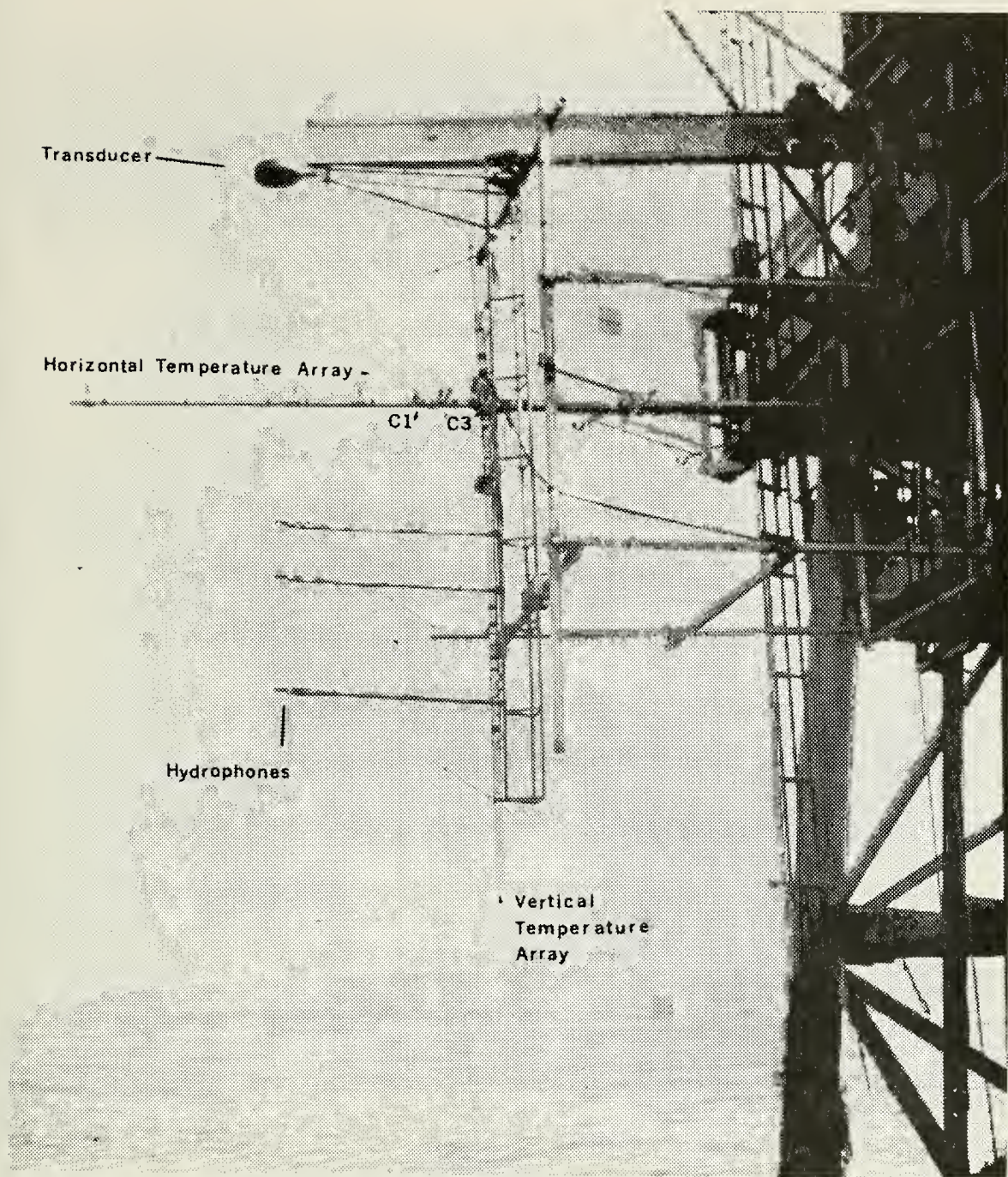


Figure 8. - Instrumentation mounted on frame for Run 12.



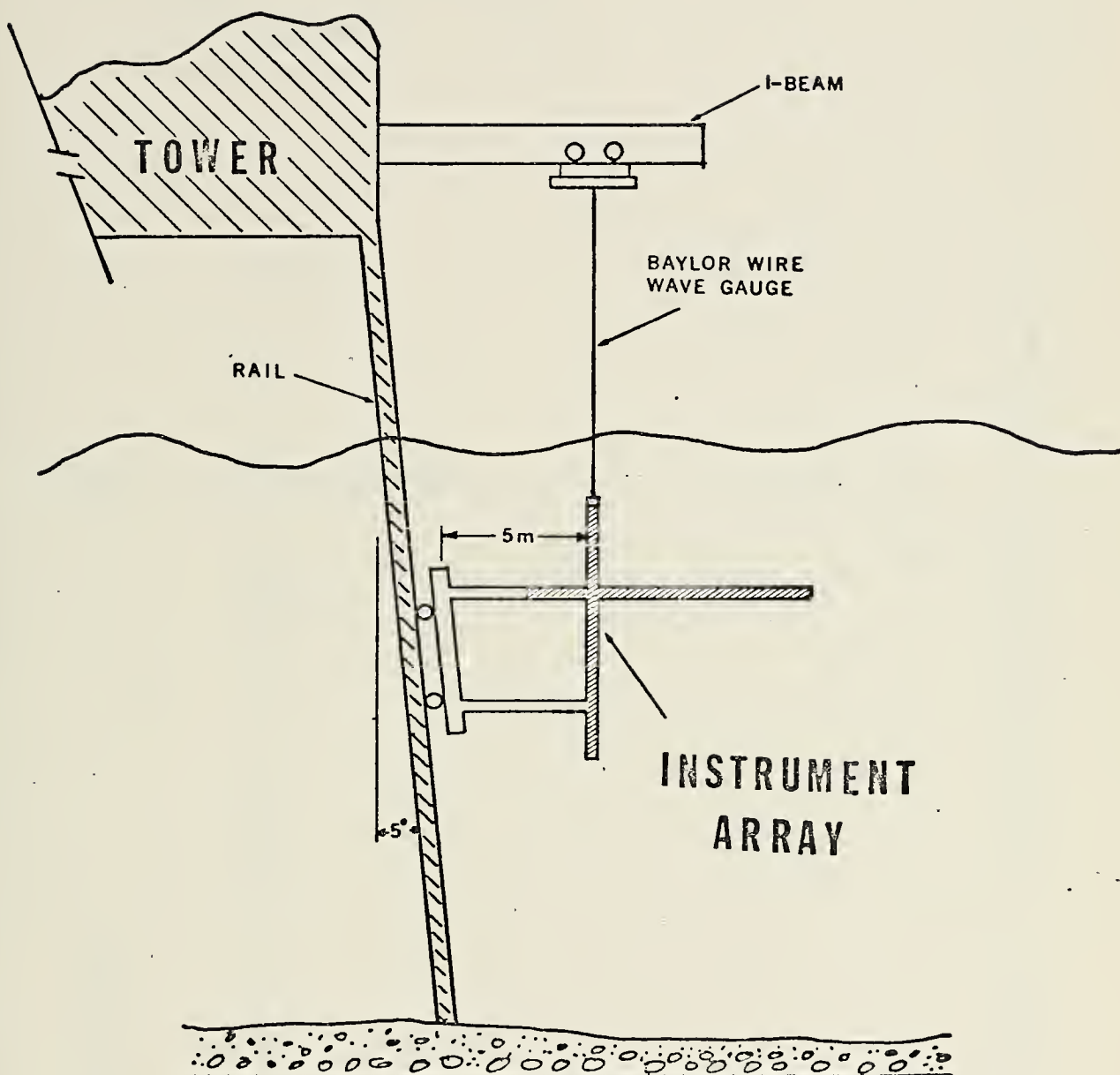
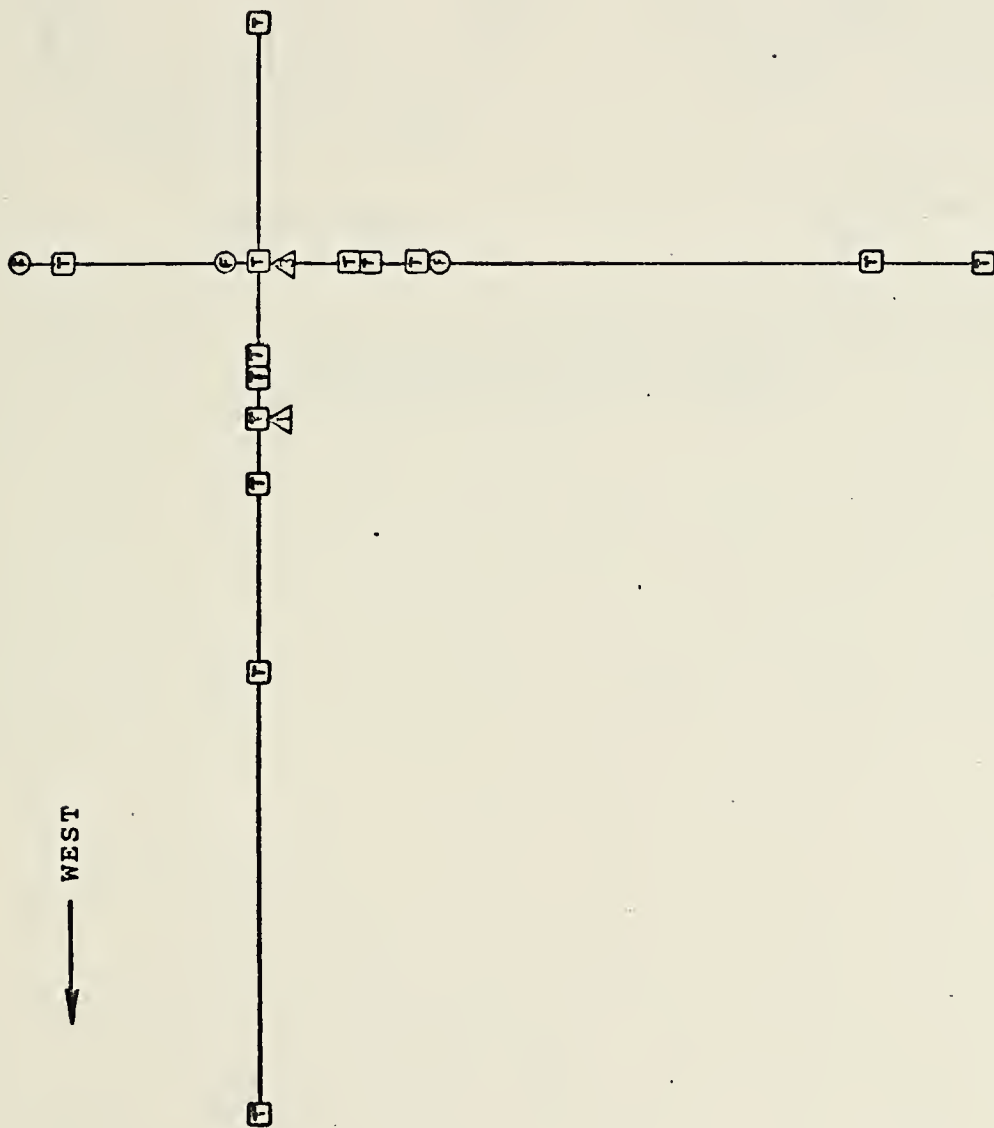


Figure 9. - Schematic of instrument arrangement on NUC Tower.





WEST  
←



Instrument Key  
 △ - Conductivity  
 □ - Thermistor  
 ⊙ - Flow Sensor

Scale : 1"=58 cm

Figure 10. - Relative positions of instruments on frame (Side view).



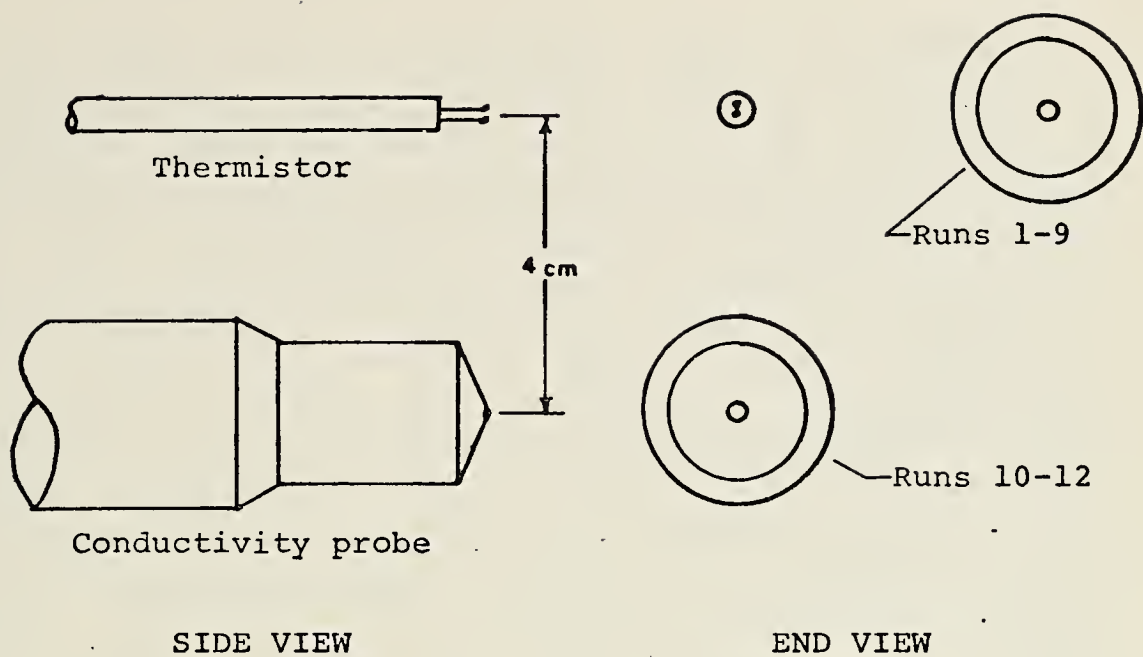


Figure 11. - Relative arrangement of conductivity probe and associated thermistor.





### C. EXPERIMENTAL PROCEDURES

For each run the instrument frame was lowered to a selected depth to provide data under a variety of conditions, such as above, below and in the thermocline as determined by a bathythermograph trace made prior to each run. At the beginning of each run the instruments were adjusted for proper operation prior to commencing recording. Flow through each conductivity probe was adjusted to approximately 0.5 to 1.0 ml/sec. The conductivity instruments were nulled to zero to allow maximum variation without exceeding the input voltage limit of the tape recorders. The null point resistance was determined at this time by momentarily inserting a decade box in place of the probe. With instruments operating properly the recorders were started. Start and stop pulses were placed simultaneously on one channel of each recorder to provide synchronization of the data records during data analysis. Other data was taken as summarized in Table II. The runs varied in length from 30 minutes to over an hour.

At the conclusion of each run a sample was obtained of the seawater which had collected in the 20 liter bottle. These samples were later analyzed for salinity using a bench salinometer to provide an average salinity for later calculations. A total of 12 runs were conducted over three days.

### D. NOTES ON RUNS

For runs 1 through 7, conductivity probe No. 2 behaved erratically. The reason for this was later determined to be due to a grounding in the probe wiring after exposure to seawater for more than an hour. This probe was then replaced with the third conductivity probe but, upon



lowering, the wire to this new probe was broken at a splice. It was not until after run 9 that the splice was repaired and the probe operated satisfactorily for the remainder of the runs.

Probe No. 1 was in operation during all runs. however its output was observed to change in a manner more similar to the wave pattern than to the observed temperature variations. Even when temperature was almost constant, probe No. 1 still displayed periodic fluctuations. While it is possible that this was actually due to changes in salinity, the magnitude and periodicity did not make it probable. Further, after run 5 the null resistance was observed to decrease from about 800 ohms to 300 to 400 ohms for the remainder of the runs.

Subsequent investigation in a wave tank at the U.S. Naval Postgraduate School has shown that with the probe in a horizontal position it is relatively easy to trap air bubbles inside the probe. If these bubbles remain under the inner sensing electrode the voltage output will fluctuate with the wave periodicity. If the bubbles are removed from the sensing area the output steadies and is no longer wave dependent. It is felt that air trapped in the probe was responsible for the poor indication of conductivity by probe No 1. If the probe had been placed in a vertical position rather than horizontal, the problem would have been eliminated. Either because probes No. 2 and No. 3 were mounted slightly non-horizontal or their individual construction made bubble entrapment different, they did not seem to suffer from the same problem.



TABLE II

## ENVIRONMENTAL DATA

Run	Winds		Seas		Swell		Surface		Thermocline		Instrument		Average	
	spd/Dir.	Ht/Dir.	Ht/Dir.	m/°	Ht/Dir.	m/°	Temperature	°C	Depth	m	Depth	m	Salinity	‰
10	10/278	0.2/300	1.0/270	13.62	0.0	5.33	33.648							
11	11/280	0.2/310	1.0/270	13.72	13.8	7.55	33.653							
12	11/292	0.2/310	1.0/270	14.16	10.4	10.48	33.666							



## V. DATA REDUCTION

Upon return to the U.S. Naval Postgraduate School the data tapes were first transcribed to a rectilinear 8 channel strip chart recorder. This provided a preliminary view of all 28 channels of data. From this overall view it was determined that some runs would be more profitable to analyze than others.

Next the selected runs were converted from analog to digital form. This was accomplished using a hybrid combination of a Ci 5000 Analog Computer and a Zerox Data System Model 9300 Digital Computer. During the process 7 channels at a time were digitized with each channel being separately filtered to remove any extraneous signals such as 60 hz noise picked up in recording or playback. An eighth channel was used for the start pulse to ensure synchronization of all 28 digitized data channels. The seven filters were tested to see that they were well matched to produce the same relative phase shift for all frequencies to be analyzed. Signal processing playback was at 7 1/2 ips or twice the recording speed. The filters were set to lowpass below 20 Hz so that real-time filtering was at 10 Hz, or below the real time Nyquist frequency of 12.5 Hz determined by the digitization rate of 50 samples per second. It was later discovered that the filters used were not perfectly matched so that false phase shifts were indicated between some records. Because of this, the data was redigitized without the filters. After digitizing, the data was then transcribed from 7 to 9 track digital tape using the Postgraduate School's IBM Model 360/67 Digital Computer. All subsequent analysis was conducted with this computer.





## VI. DATA ANALYSIS

Based on preliminary analysis of strip chart recordings, runs 1,2,3,6,10,11 and 12 were selected to be further analyzed. In general these runs were chosen because they provided active variations of the data due to surface and internal wave action. This would allow a spectral analysis of the data. The objectives of the analysis were to:

1. Determine the energy density distribution as a function of frequency for the data recorded from the conductivity instruments and associated thermistors.

2. Determine the spectral relationships between conductivity and temperature and how they are related to the wave and velocity structure.

3. Compute salinity from conductivity and temperature and perform spectral analysis on the resultant data to determine if it is a reasonable representation of the salinity microstructure.

With these results it should then be possible to determine how well the conductivity probes measured salinity variations which could in turn be used in the analysis of sound microstructure.

### A. METHODS OF ANALYSIS

The data analysis was performed using the Naval Postgraduate School's IBM Model 360/67 Digital Computer.



## 1. Data Conditioning

The first step of the analysis procedure was to digitally filter the data using an inverse transform filter [Davidson 1970]. The weighting function is given by:

$$h_n = \frac{\Pi [ \sin(w_t n \Delta t) + \sin(w_c n \Delta t) ]}{2n \Delta t [ \Pi^2 - (w_t - w_c)^2 n \Delta t ]}$$

where

$h_n$  =  $n^{\text{th}}$  weight

$w_c$  = cutoff frequency

$w_t$  = terminal frequency

$n$  =  $n^{\text{th}}$  weight of  $N$  weights

$\Delta t$  = time step interval

For this analysis, cutoff frequency was chosen as 2.0 Hz, terminal frequency as 4.9 Hz and number of weights as 15. This would provide a satisfactory filter below 1.5 Hz with minimum computation. The transfer function for this filter is shown in Figure 12.

The data was next decimated by a factor of five to reduce the data to a workable level. This yielded a final sampling rate of five samples per second. The Nyquist frequency associated with this sample rate is 2.5 Hz.

After decimation, the data was multiplied by a calibration factor to convert the data from voltage to actual units such as ohms or degrees centigrade for conductivity and thermistor instrument records respectively. The average, standard deviation and variance of the data were computed and the linear trend and average removed.



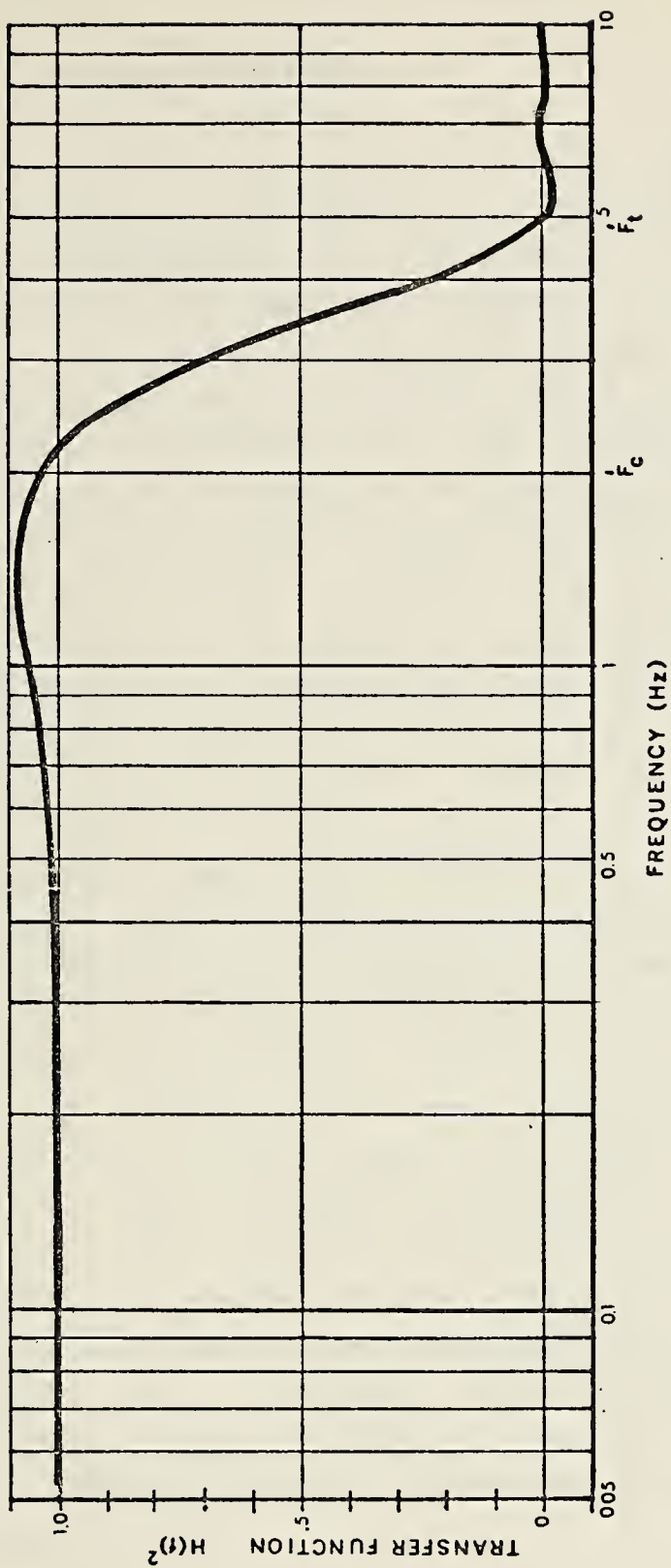


Figure 12. - Inverse filter transfer function for cutoff frequency of 2.0 Hz and terminal frequency of 4.9 Hz.



## 2. Spectral Analysis

Spectral analysis of the data records was accomplished by calculating a covariance function and Fourier transforming it to obtain a spectrum of energy density. A ten percent lag was used to provide statistical reliability. A Parzen window was applied to the covariance function to correct for a finite record length. The results of this analysis are the autospectrum and the autocorrelation function for an individual data record. The autospectra were normalized for comparison purposes.

From pairs of data records the coherence and phase relationships were computed. A coherence of one is perfect correlation, i.e., a change in one record is matched by a corresponding equivalent change in the other record. Phase indicates the delay between records for this change to occur.

Generally only the frequencies up to 1.0 Hz were examined. In this region the dominant forcing mechanism is due to surface waves. Turbulence also becomes noticeable in this region and tends to dominate at higher frequencies.

The record length was chosen to provide enough data points to resolve the lowest wave frequencies expected. This requires a record length of at least ten times the wave period in order to obtain any statistical reliability. By this criterion a minimum record length of 200 seconds is necessary to resolve a wave with period of 20 seconds. A longer length would have provided more reliability for stationary data. However, due to the passage of internal waves the data was not stationary except over short records. Thus a compromise of 400 seconds was normally used for data analysis.





### 3. Salinity Synthesis

Salinity was computed in the time domain from time records of conductivity and associated temperature using equation (6). Temperature and salinity coefficients were obtained from Higgin's nomographs based on the average temperature and salinity for the run. These coefficients are themselves functions of temperature and salinity, but to a good first approximation, the second order effects caused by variations of temperature and salinity are negligible. Thus only one value of the coefficient was needed for each run.

The variations in temperature,  $\Delta T$ , and in conductivity,  $\Delta \sigma$ , were determined from the respective records about the mean value. The linear trends were not removed from these records so that trends of salinity could be analyzed. With a time record of salinity computed, the spectral analysis of salinity and its coherence and phase relationships with temperature and conductivity were accomplished in the manner described above.

#### B. RESULTS OF ANALYSIS

The results of spectral analysis indicated that of the seven selected runs, 1,2,3 and 6 were not suitable for a more detailed analysis of conductivity. In particular, conductivity probe No. 2 displayed noise over the entire spectrum. As previously mentioned, this was due to a short in the probe wiring. Conductivity probe No. 1 appeared to be inoperative during all twelve runs due to air entrapment in the probe tip.

Runs 10, 11 and 12, however, did appear to provide good data from the third probe which was substituted for conductivity probe No. 2. Runs 10 and 12 exhibit large



variations in conductivity and temperature when internal waves moved the thermocline into the vicinity of the instrument sensors. Run 11 is interesting because it is relatively quiet with little variation in the data record since it recorded conditions above the thermocline. Figures (13), (14) and (15) show the spectral analysis results of conductivity instrument No. 3 and its associated temperature. Phase and coherence relationships between these two records are also shown.



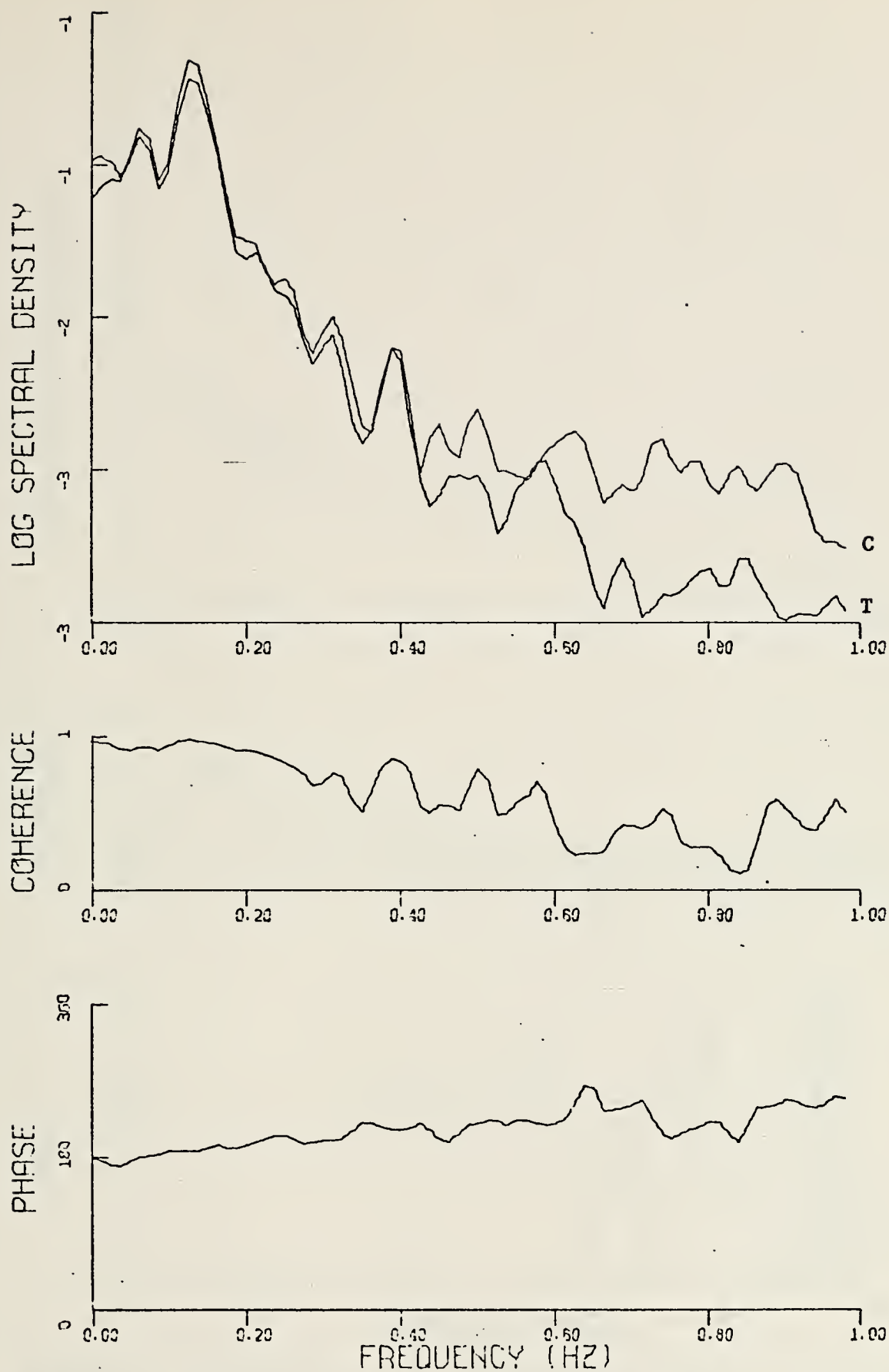


Figure 13. Conductivity and temperature spectra, coherence and phase - Run 10.



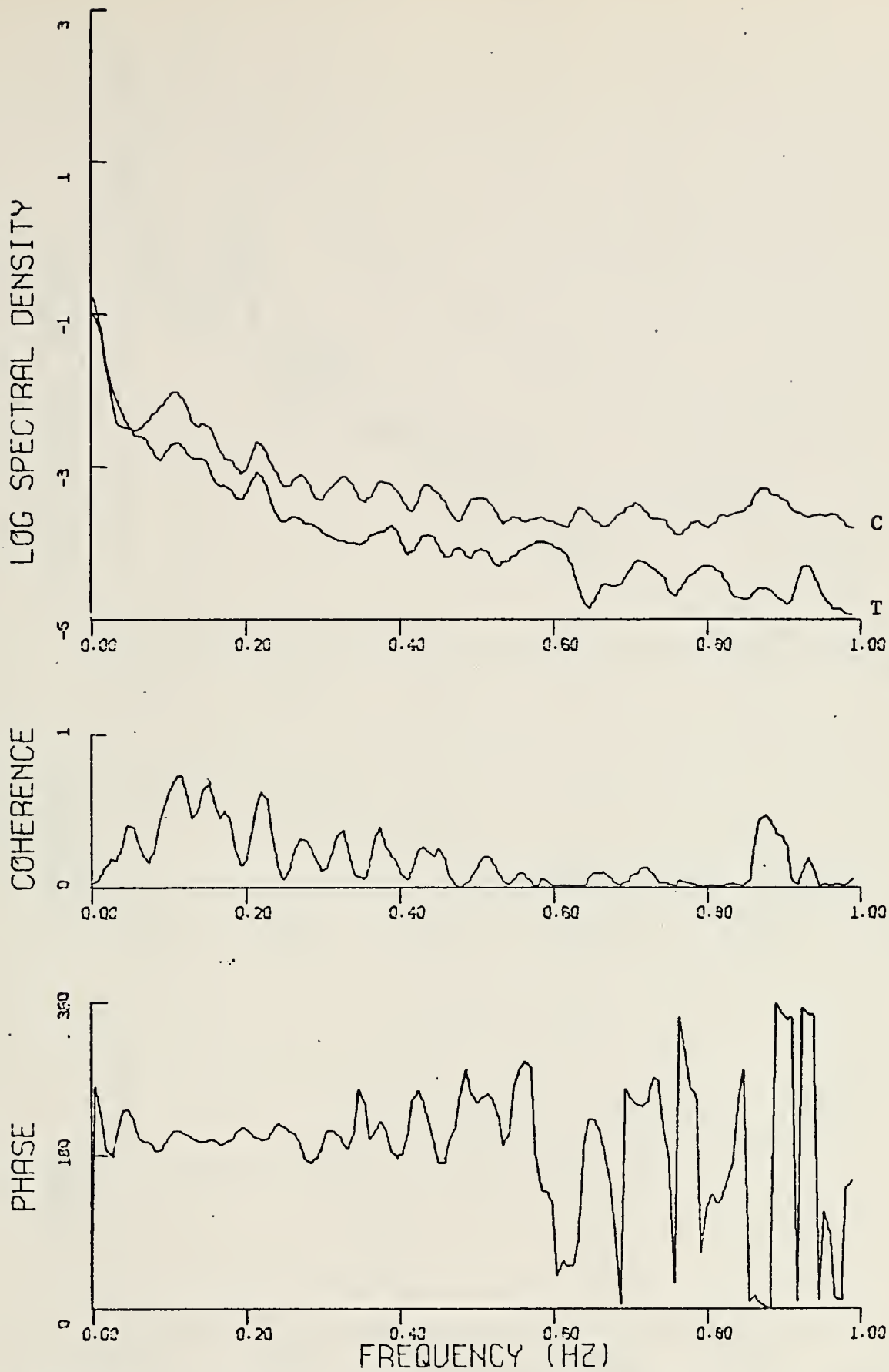


Figure 14. Conductivity and temperature spectra, coherence and phase - Run 11.





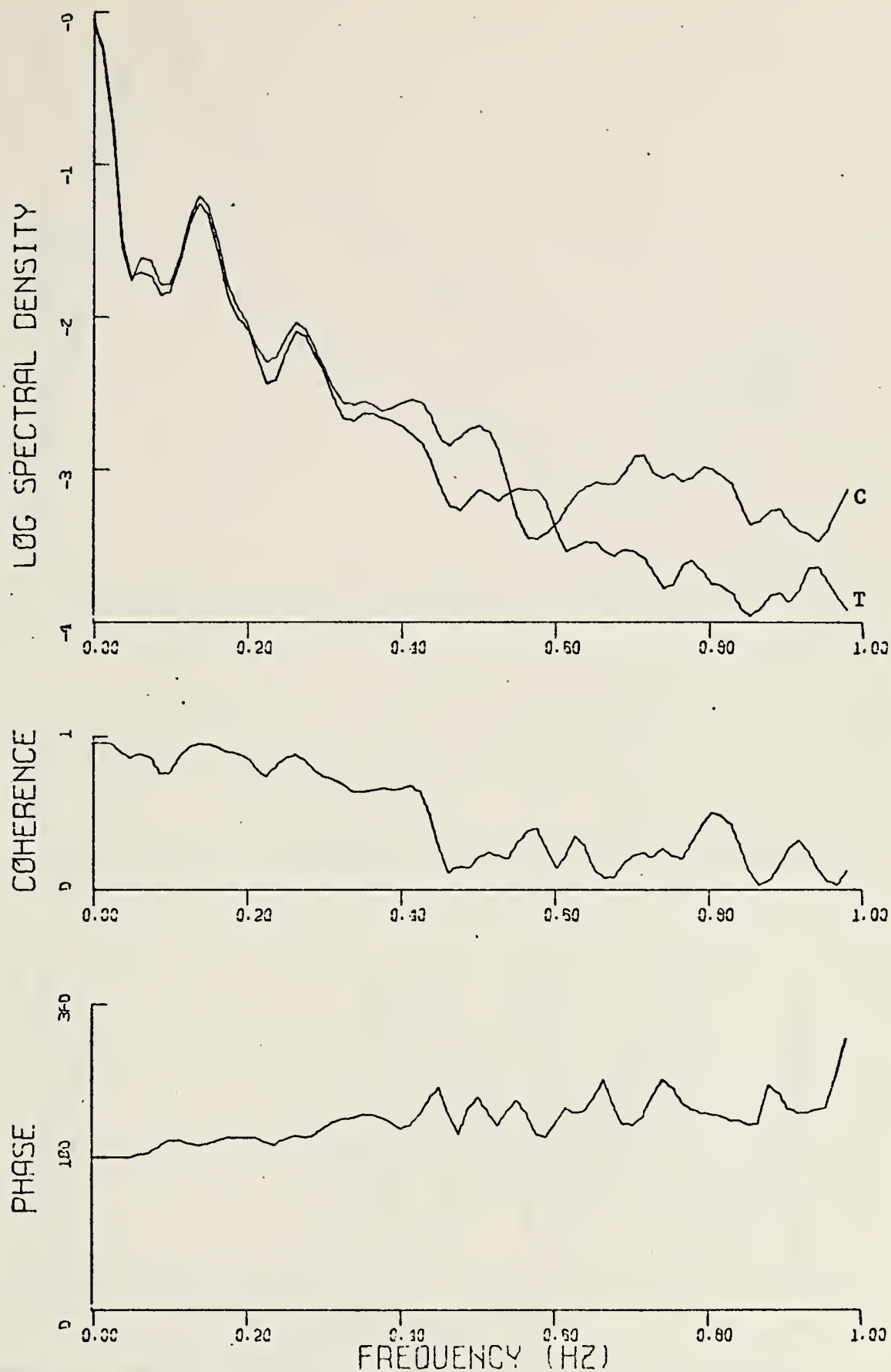


Figure 15. Conductivity and temperature spectra, coherence and phase - Run 12.



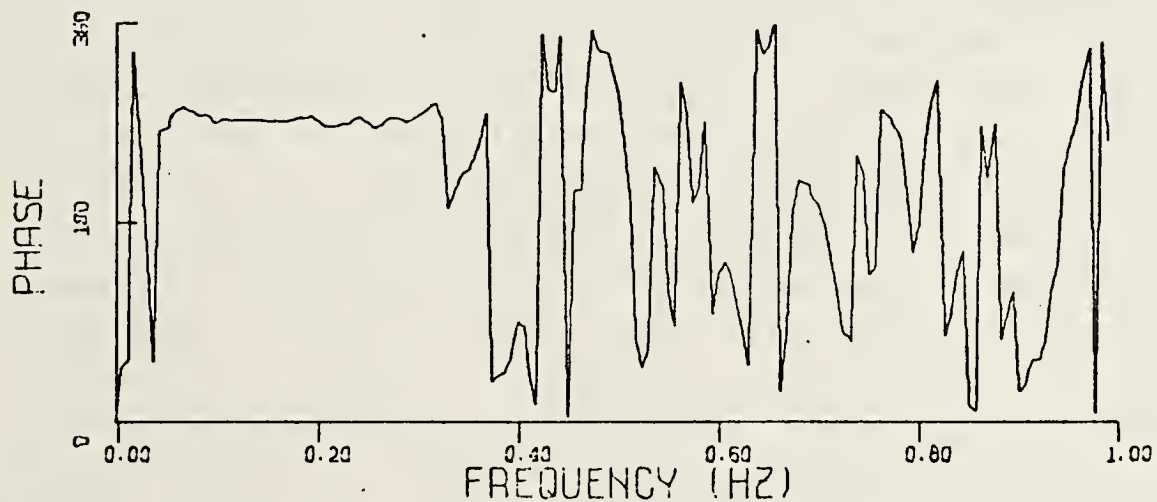
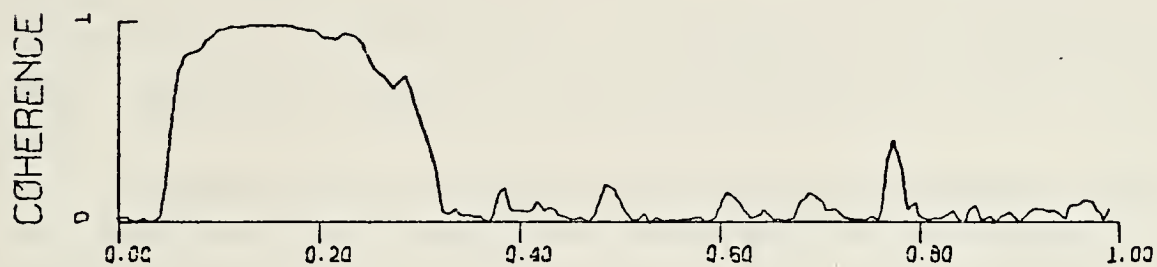
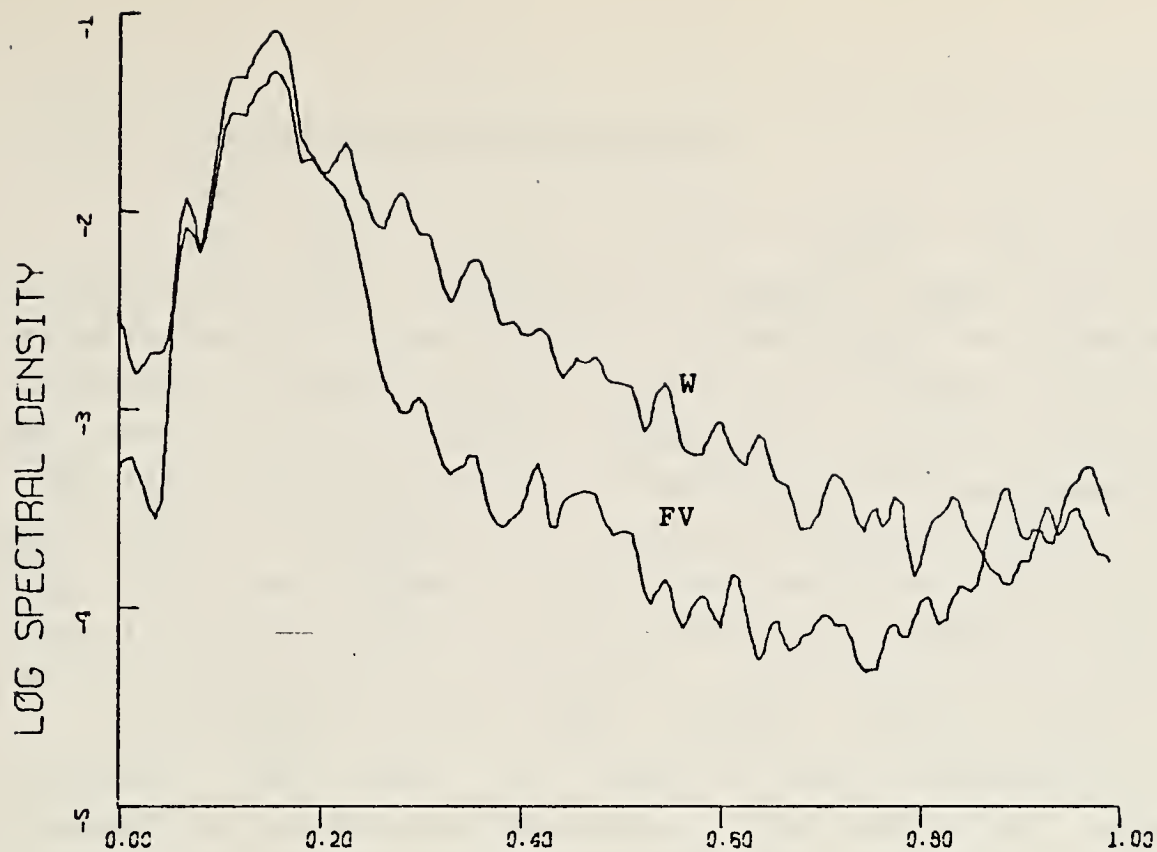


Figure 16. Spectra of waves and vertical fluid particle velocity - Run 12.



## 1. Conductivity And Temperature

For runs 10 and 12, the spectra for both conductivity and temperature display peaks at the frequencies of .07 and .125 Hz corresponding to observed predominant wave periods of 14.2 and 8.0 seconds. Spectra of waves and the vertical component of fluid particle velocity at the depth of the conductivity probe are compared in Figure 16. Periods of 4.0 and 2.5 seconds (.25 and .4 Hz) are also evident in both conductivity and temperature spectra, but the origin of these peaks is uncertain. Above 0.4 Hz the spectra of conductivity and temperature separate.

Run 11 spectra do not very clearly display the wave periods. The reason for this is the relatively small temperature and salinity gradients in the well mixed region above the thermocline. As with runs 10 and 12, it also displays a separation of the spectra of conductivity and temperature. Furthermore, the separation of conductivity and temperature spectra is not as clear as in runs 10 and 12.

An examination of plots of log spectral density versus log frequency suggests why this separation occurs. For conductivity the slope of the plot in the region above 0.4 Hz is about  $-5/3$  (Fig. 17). This is what Kolmogoroff's theory predicts for the slope of the turbulent kinetic energy spectrum in the inertial sub-range. Since conductivity and temperature are both passive scalar quantities, it might be expected that at these frequencies their spectra would be similar. However, the slope for temperature is steeper, about  $-8/3$  (Fig. 18). This steeper slope may be caused by the large time constant for the temperature measuring instrument (250 msec for this particular thermistor). The effect would be to reduce energy density at higher frequencies due to the low pass filtering action of the time constant. The conductivity



probe with a time constant of about 8 msec does not suffer this degradation, hence the divergence of the spectra at higher frequencies.

The coherence between conductivity and temperature decreases above 0.5 Hz. This is caused not only by the difference in time constants, but also by the decoupling of conductivity and temperature due to their physical separation of 4 cm. Run 11 does not display coherence as well as runs 10 and 12 because of the lower energy in the region where the higher coherence is expected. This decoupling can also be seen by comparing two temperature records where the thermistors were vertically separated by 5 cm (Fig. 19).

The phase relationship between conductivity and temperature displays a slowly increasing phase difference from  $180^\circ$ . This is particularly noticeable in Figures 13 and 15. A  $180^\circ$  phase shift is expected for no time delay between the two records since as temperature increases, resistance decreases proportionately in accordance with equation (6). If the measuring devices are physically separated, a phase shift will occur due to the time delay for the change between the two. This is what is seen. This change of phase shift is also almost exactly duplicated by the two thermistors separated by 5 cm. A constant zero degree phase shift would be expected for these thermistors if they were measuring at the same point.

From the results of the spectra, coherence and phase relationships, it appears that the conductivity instrument functioned properly for runs 10 through 12. This was encouraging since such reasonable conductivity data combined with the temperature data allowed computation of salinity information.





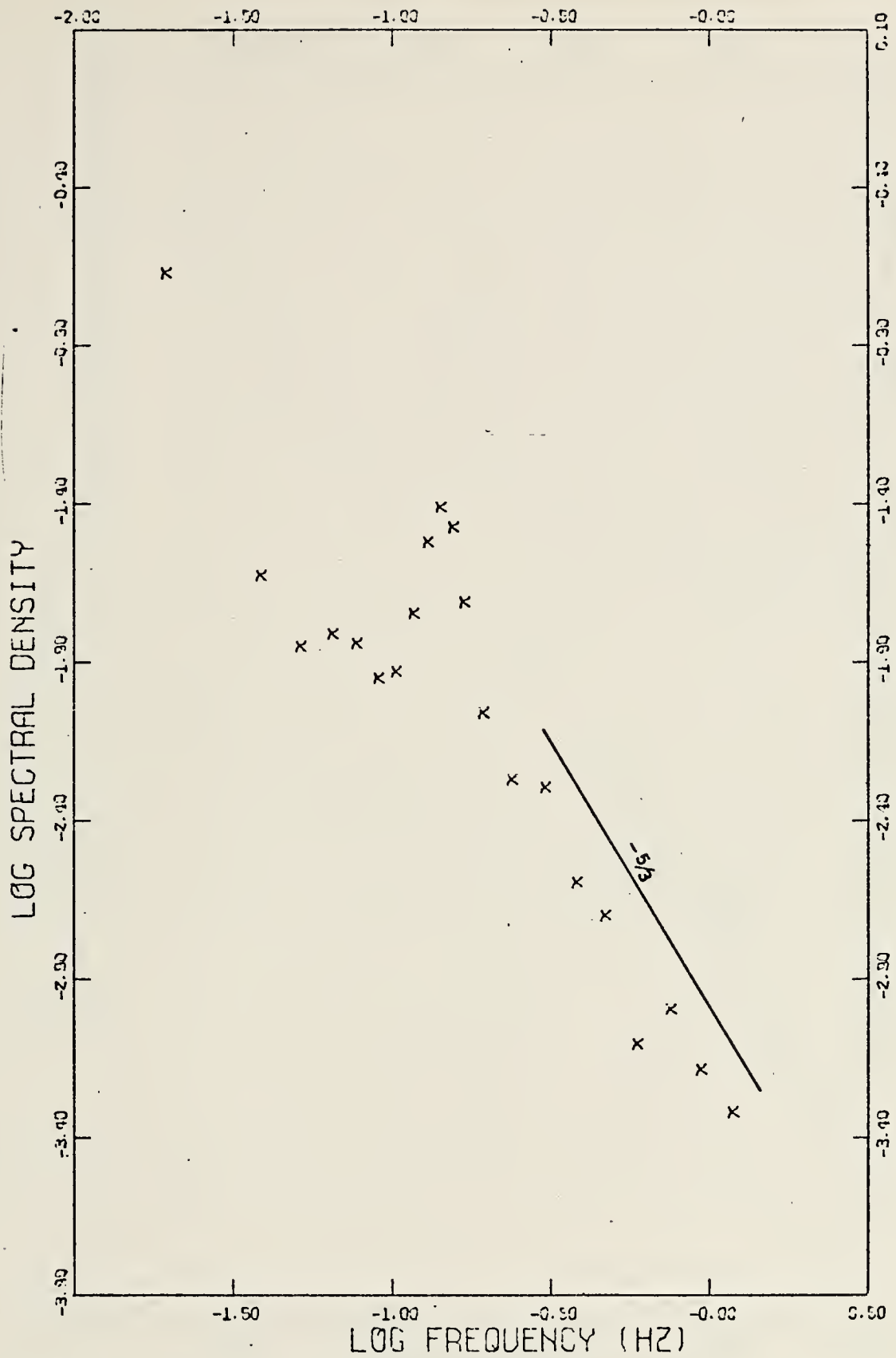


Figure 17. Log-log plot of conductivity spectrum - Run 12.



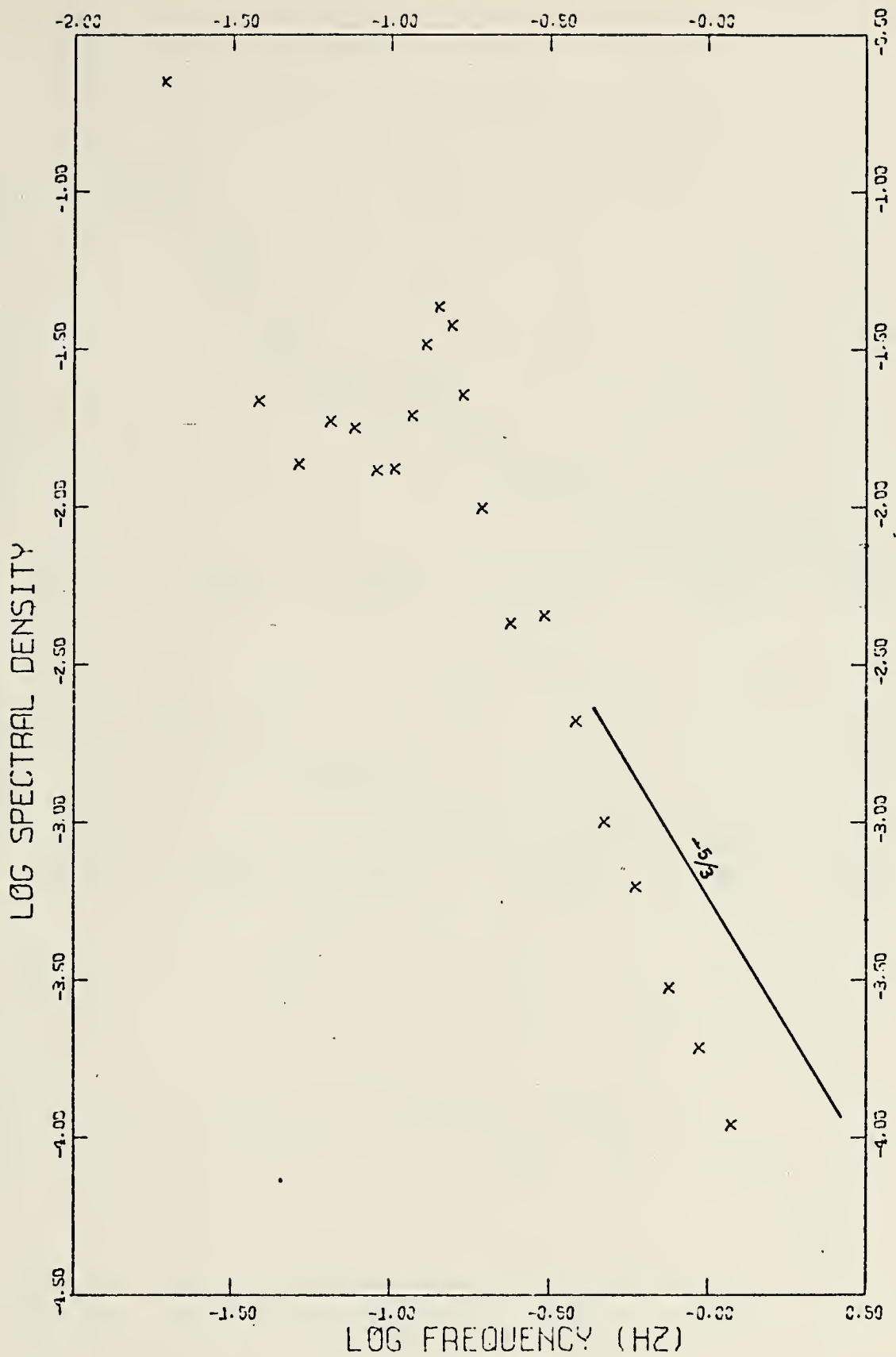


Figure 18. Log-log plot of temperature spectrum - Run 12.



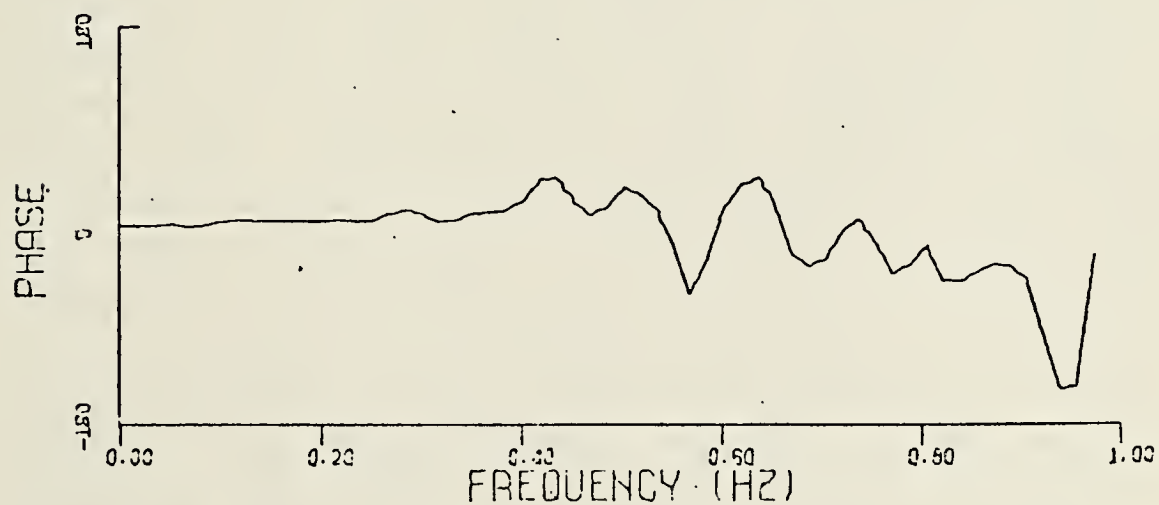
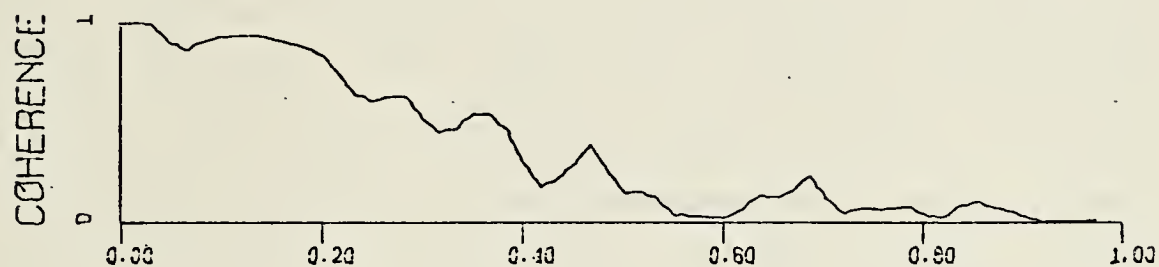
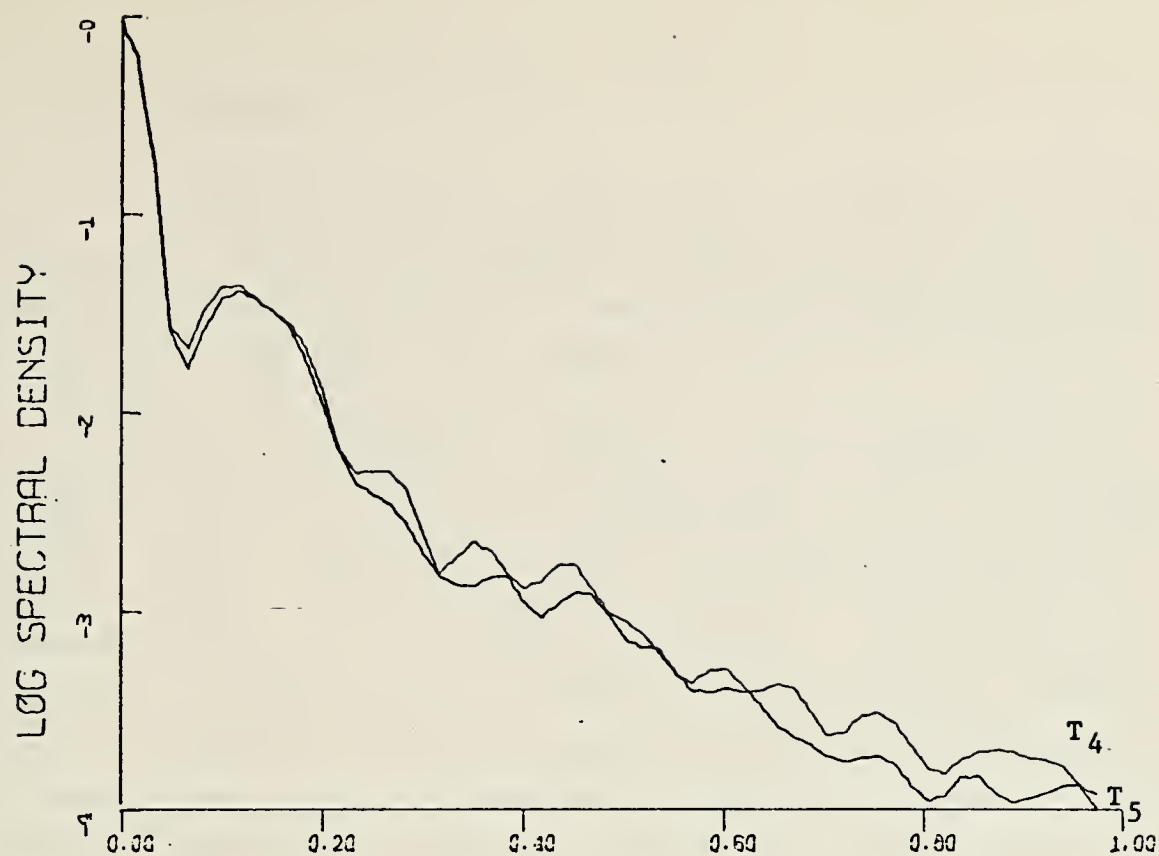


Figure 19. Spectra of temperatures vertically separated by 5 cm - Run 12.



## 2. Salinity

Temporal salinity records were synthesized for runs 10 and 12 from data records of conductivity probe No. 3 and its associated thermistor. These salinity records were then subjected to the same spectral analysis. Results are displayed in Figures 20 to 23.

Salinity corresponds roughly to both conductivity and temperature at the lower frequencies. At the higher frequencies, coherence decreases between salinity and temperature, but increases between salinity and conductivity. This implies that at lower frequencies salinity, temperature and conductivity are equally affected by the energy producing mechanism of waves. Salinity and temperature become decoupled at higher frequencies and salinity then dominates in its effects on conductivity.

A log-log plot of the salinity spectrum indicates that the spectrum decreases at less than the  $-5/3$  theoretical slope (Fig. 24). This could either be due to the difference in the diffusivity rates of heat and salt or due to computational noise in the synthesized record. As regards the former, Batchelor [1959] described how a scalar spectrum can be expected to deviate from a kinetic energy spectrum for the case of small diffusivity. He expressed this in terms of the dimensionless ratio of  $\nu$  (the kinematic viscosity) to  $\kappa$  (the diffusivity). This ratio ( $\nu/\kappa$ ) is known as the Prandtl number ( $\sigma$ ). When the Prandtl number is large (small diffusivity), the scalar spectrum is expected to exhibit a slope of  $-1$  on a log-log plot at scales where viscosity is important. At even smaller scales where diffusivity becomes important, the spectrum should fall very steeply. The range of scales over which a slope of  $-1$  is exhibited depends on the relative magnitudes of the Prandtl numbers. The Prandtl number for salt is two orders of magnitude larger than for temperature so that the departure





from the  $-5/3$  slope could be expected to be more noticeable for the salinity spectrum than for the temperature spectrum.

In an effort to resolve whether the salinity log-log slope was due to noise or diffusivity effects, a piecewise regression plot was made of the variances of conductivity versus the variances of temperature (Figs. 25 and 26). For this plot, conductivity and temperature were changed to "equivalent salinity" using equation (6). The average variances of 16 seconds of data were determined along 800 seconds of record. If changes in conductivity were due only to changes in temperature, the variance plot points would be on a straight line at  $45^\circ$ . In actuality the least square fit of the variance points is a  $45^\circ$  line as indicated. That all data points do not fall on this line is either due to real differences caused by salinity fluctuations or due to computational noise. Hence these plots, while not resolving the question concerning salinity, do indicate that conductivity was largely temperature influenced.

The computed average variance of salinity was about .004 ppt for run 12. This compares to average variances for conductivity and temperature of .012 and .013 ppt. This also implies that temperature variations were dominant causes for the changes in conductivity.



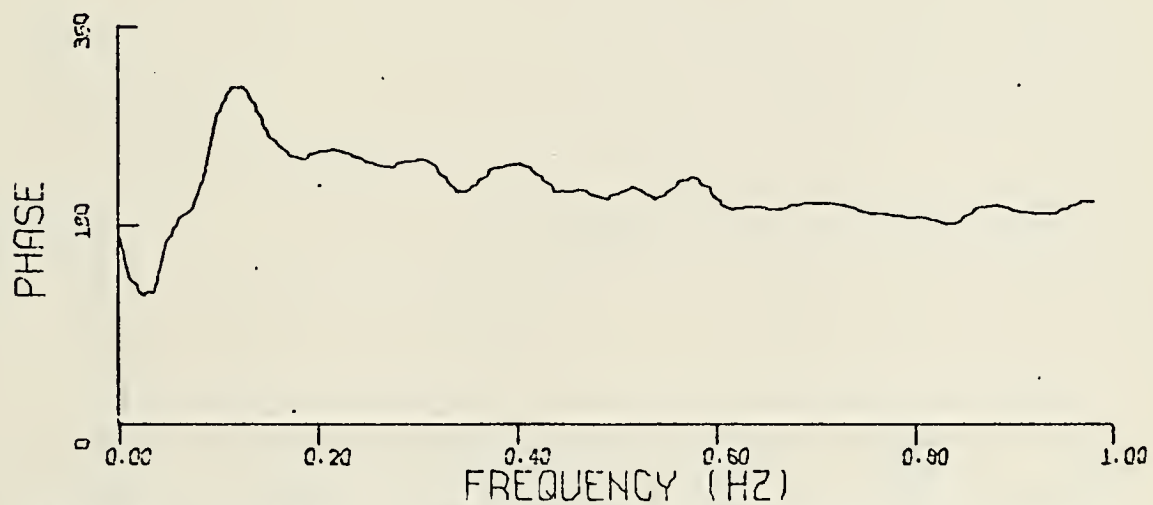
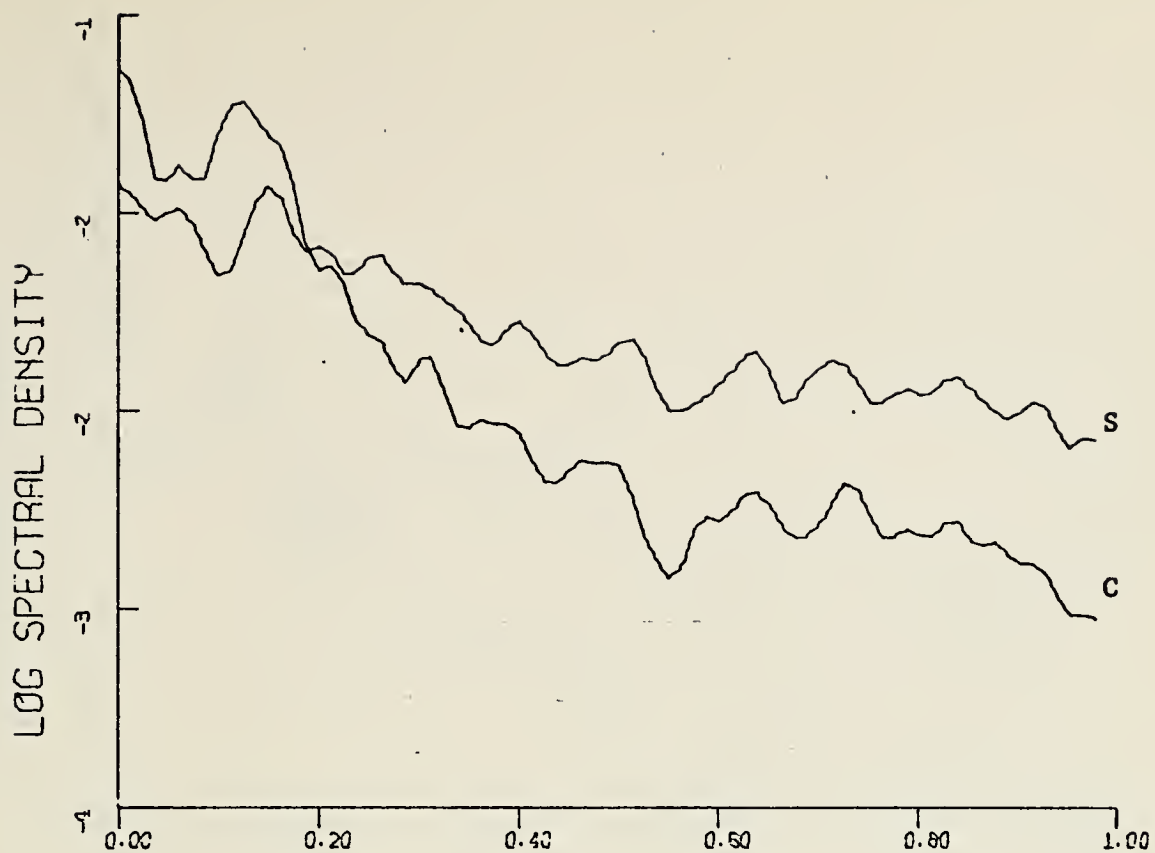


Figure 20. Salinity and conductivity spectra, coherence and phase - Run 10.



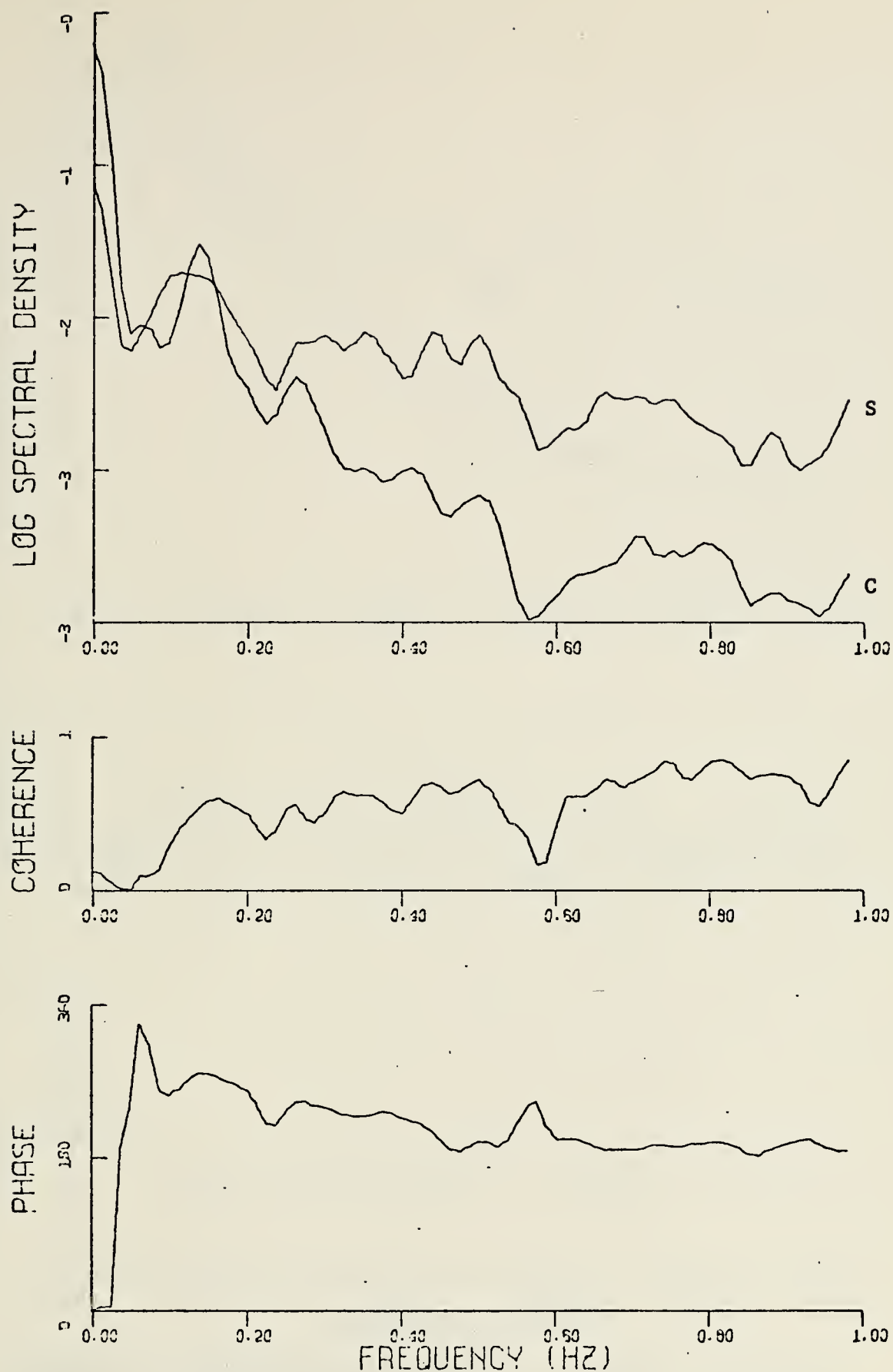


Figure 21. Salinity and conductivity spectra, coherence and phase - Run 12.



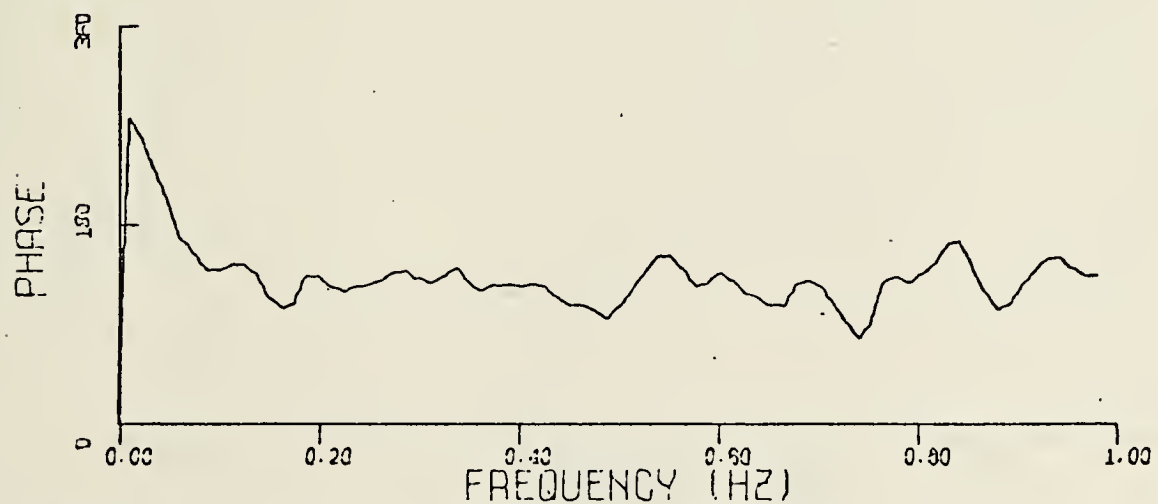
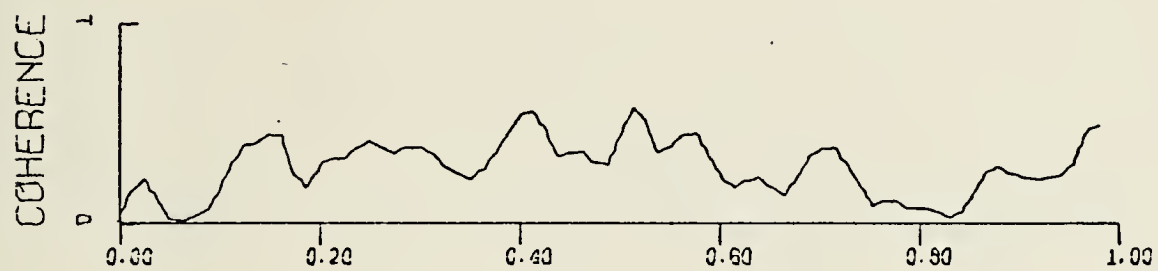
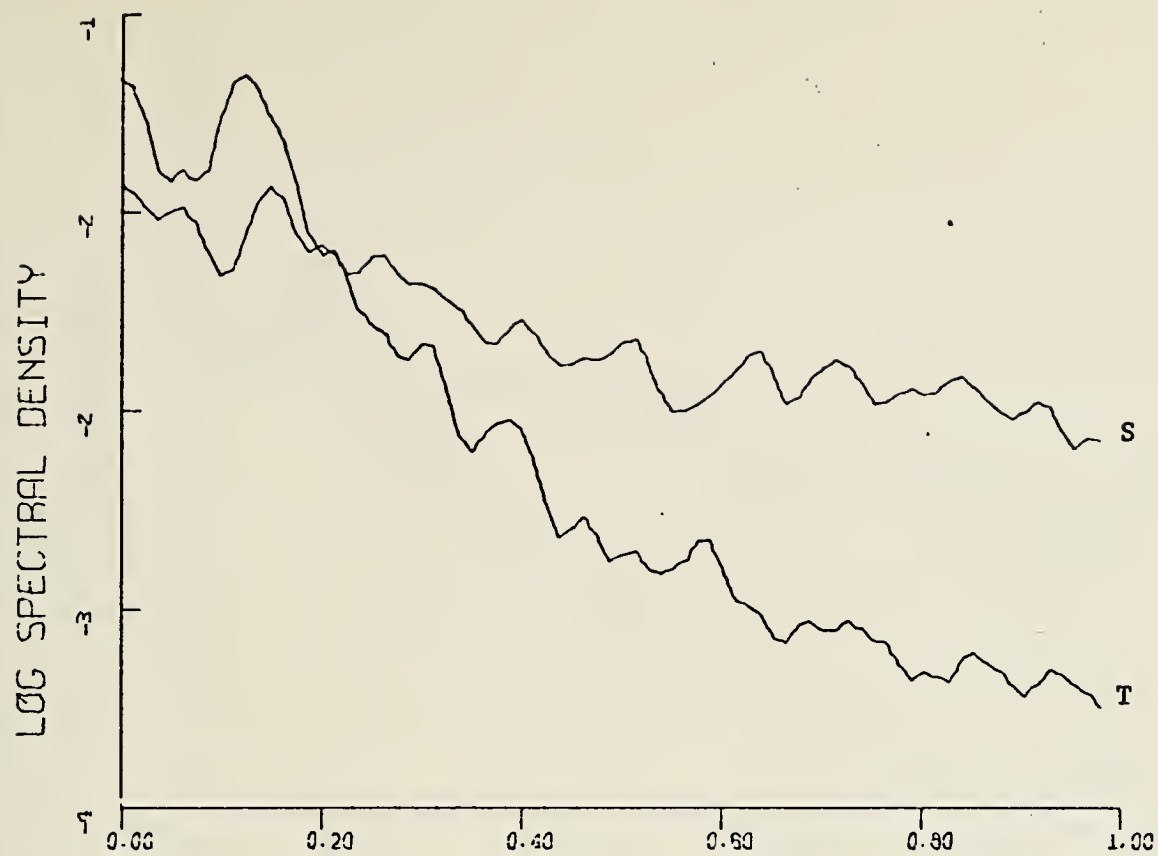


Figure 22. Salinity and temperature spectra, coherence and phase - Run 10.





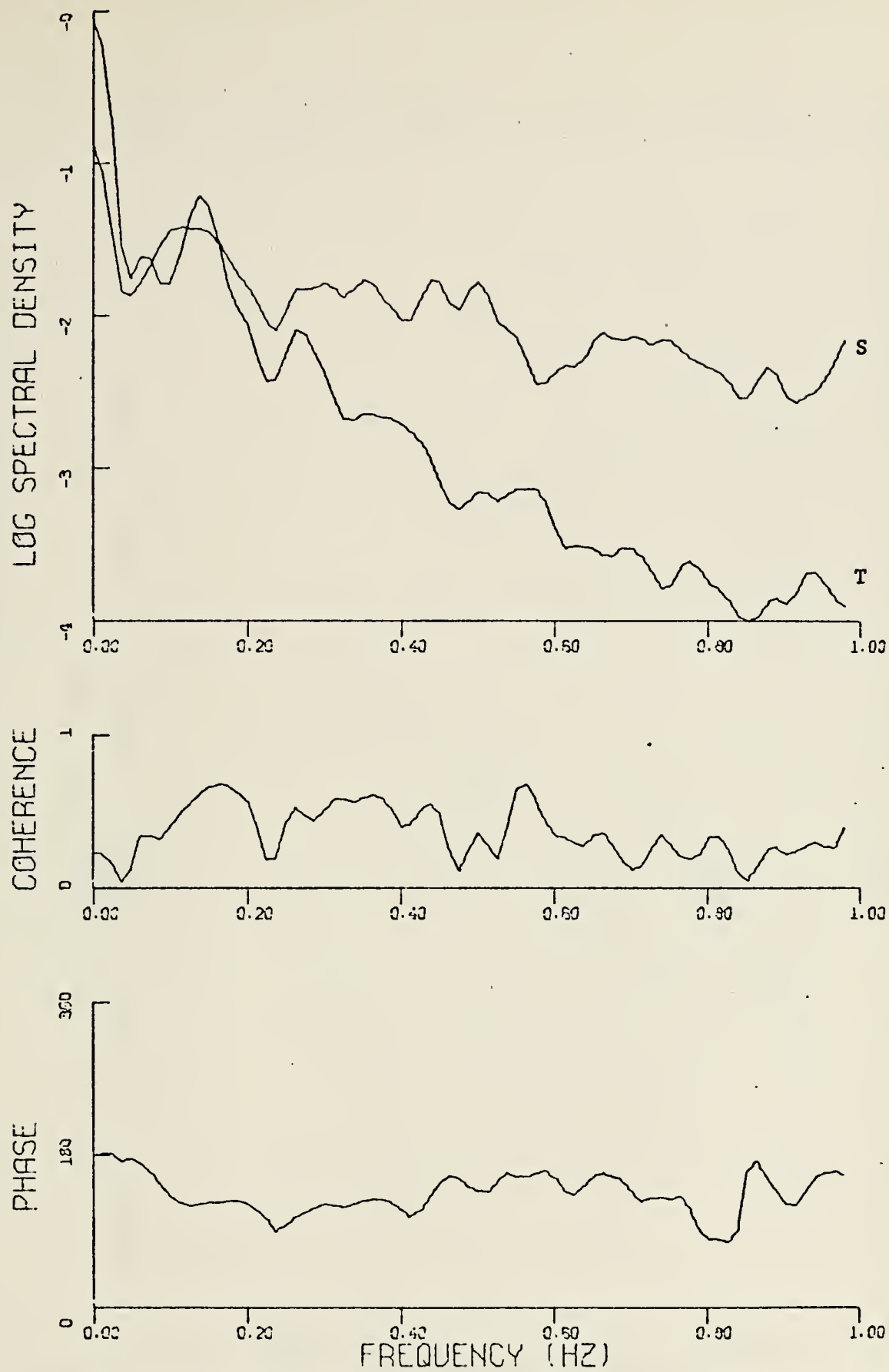


Figure 23. Salinity and temperature spectra, coherence and phase - Run 12.



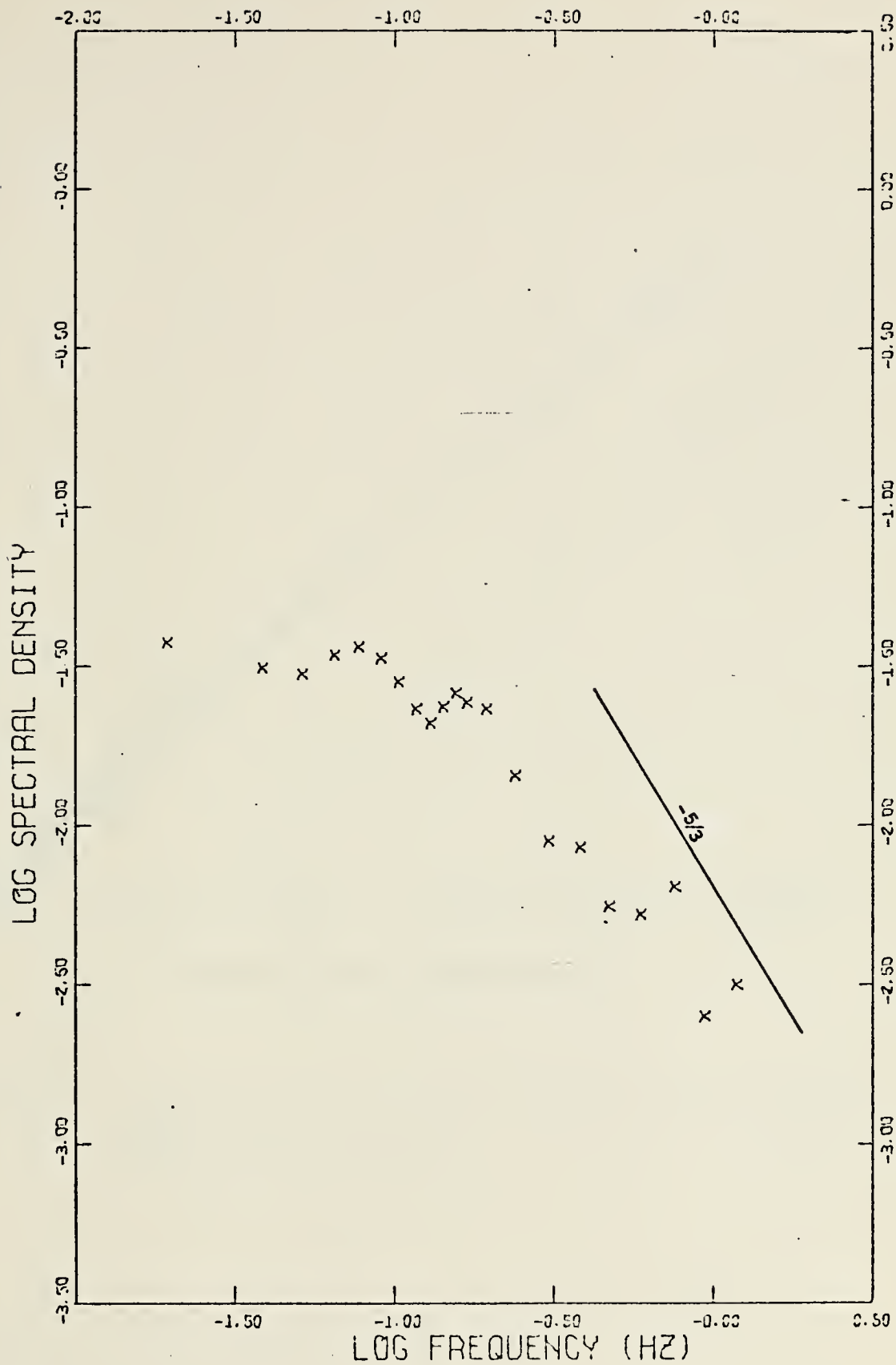


Figure 24. Log-log plot of salinity spectrum - Run 12.



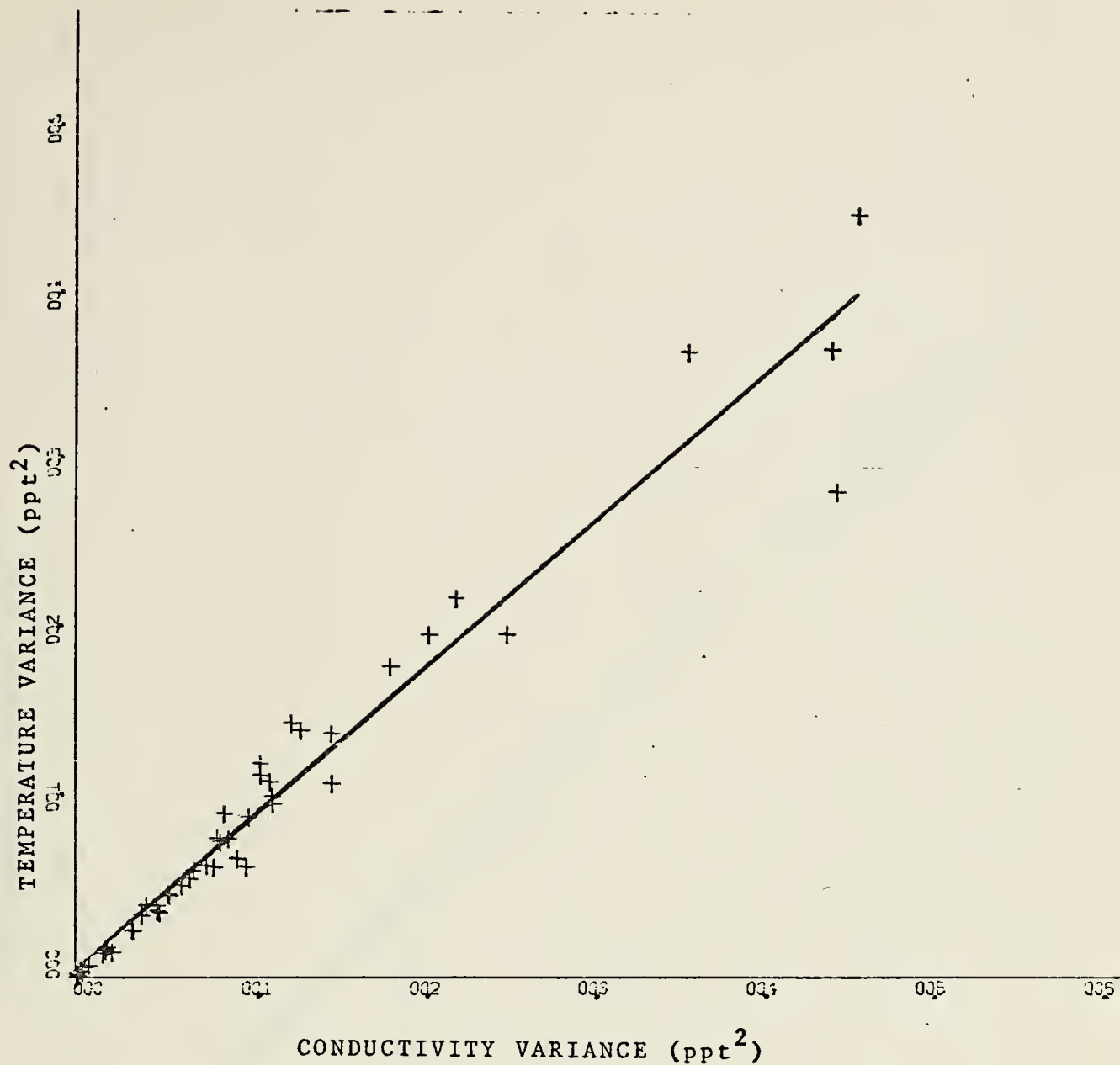


Figure 25. Regression plot of variances of conductivity and temperature - Run 10.



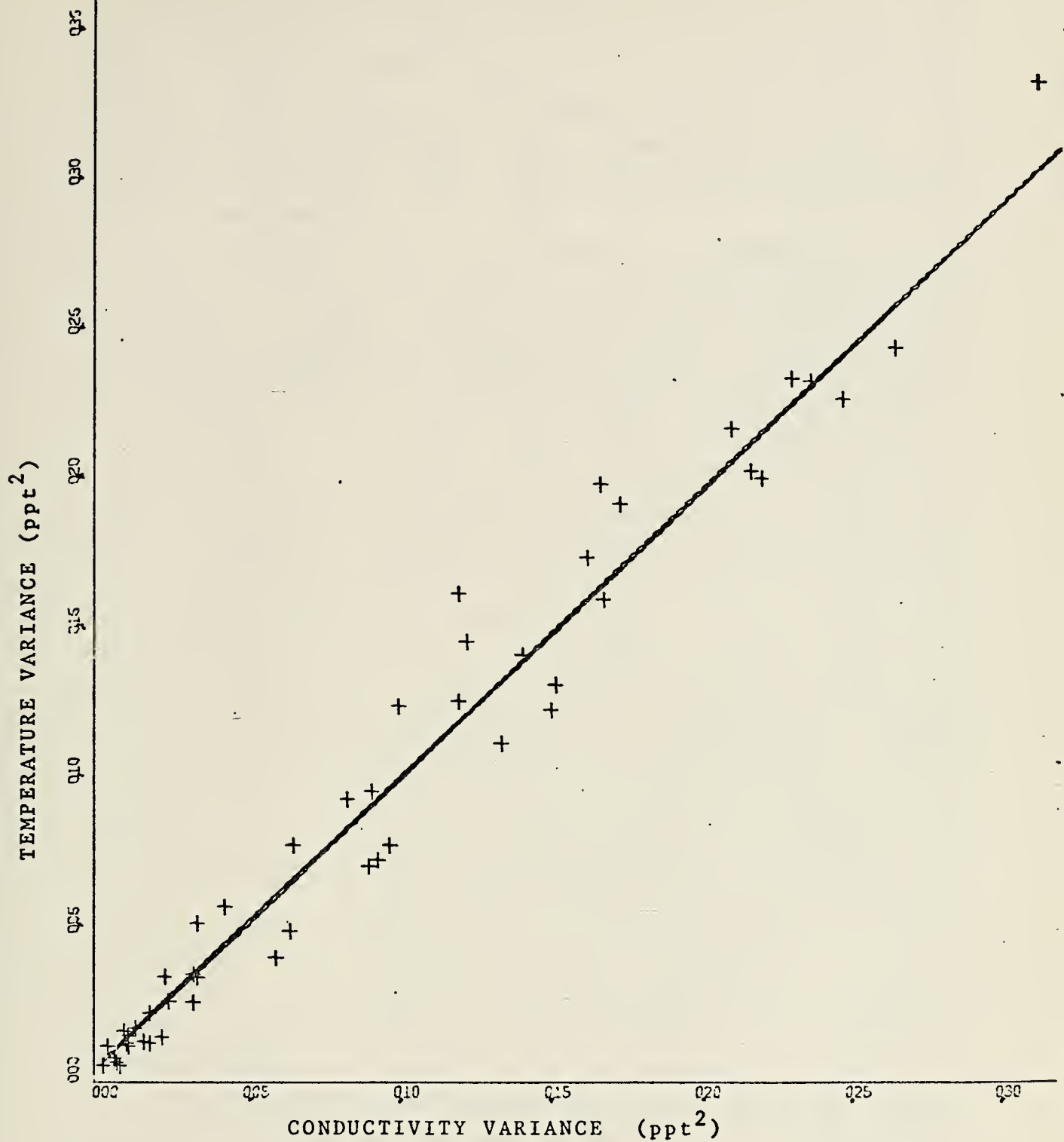


Figure 26. Regression plot of variances of conductivity and temperature- Run 12.





Because salinity was not actually measured during the ocean experiment, a plot of the record was made from the computed salinity record. Figure 27 is this time plot of salinity for run 12 and Figures 28 and 29 are the corresponding conductivity and temperature plots in equivalent salinity. All these time plots were produced with the mean removed.

Of interest is the fact that conductivity and temperature correspond very well to each other. Both demonstrate a large change as an internal wave moves past and greatly changes the temperature field. Salinity does not display this same nature of change. Instead it remains relatively flat with variations about the mean. Large salinity spikes are evident. These are not like those which occur with the STD, but rather take place over a time of several seconds. In order to determine the cause for these spikes, expanded time plots were made of these records to display the first 64 seconds (Figs. 30 to 33). When superimposed on each other, it becomes evident that the salinity spikes are largely caused by differences in the rise and fall time of conductivity and temperature. These may be seen to occur mainly at the wave periodicity. When compared to water particle vertical velocity measured in the vicinity of the conductivity and temperature instruments, it is seen that many of the large differences occur as particle velocity passes through zero. This would cause a maximum time lag between conductivity and temperature coupled changes due to the separation distance of the instruments. This in turn would cause the large salinity spikes observed at these times.

At other times in the water particle velocity cycle, however, differences between conductivity and temperature still exist. While some of this may be due to the larger time constant of temperature as compared to conductivity, it must be assumed that the rest is due to actual salinity variations.



It may also be seen that while the temperature time record is relatively smooth and wave like, that of conductivity has very small variations superimposed on the wave like structure. These variations are due to the salinity microstructure which exists to a finer scale than does temperature microstructure. The reason for this is the much smaller (factor of 100) diffusivity of temperature compared to salinity. Temperature inhomogeneities are rapidly lost due to turbulent mixing and diffusion. Salinity inhomogeneities, however, persist because of the slower diffusion process. Thus the salinity variations are, in part, real.



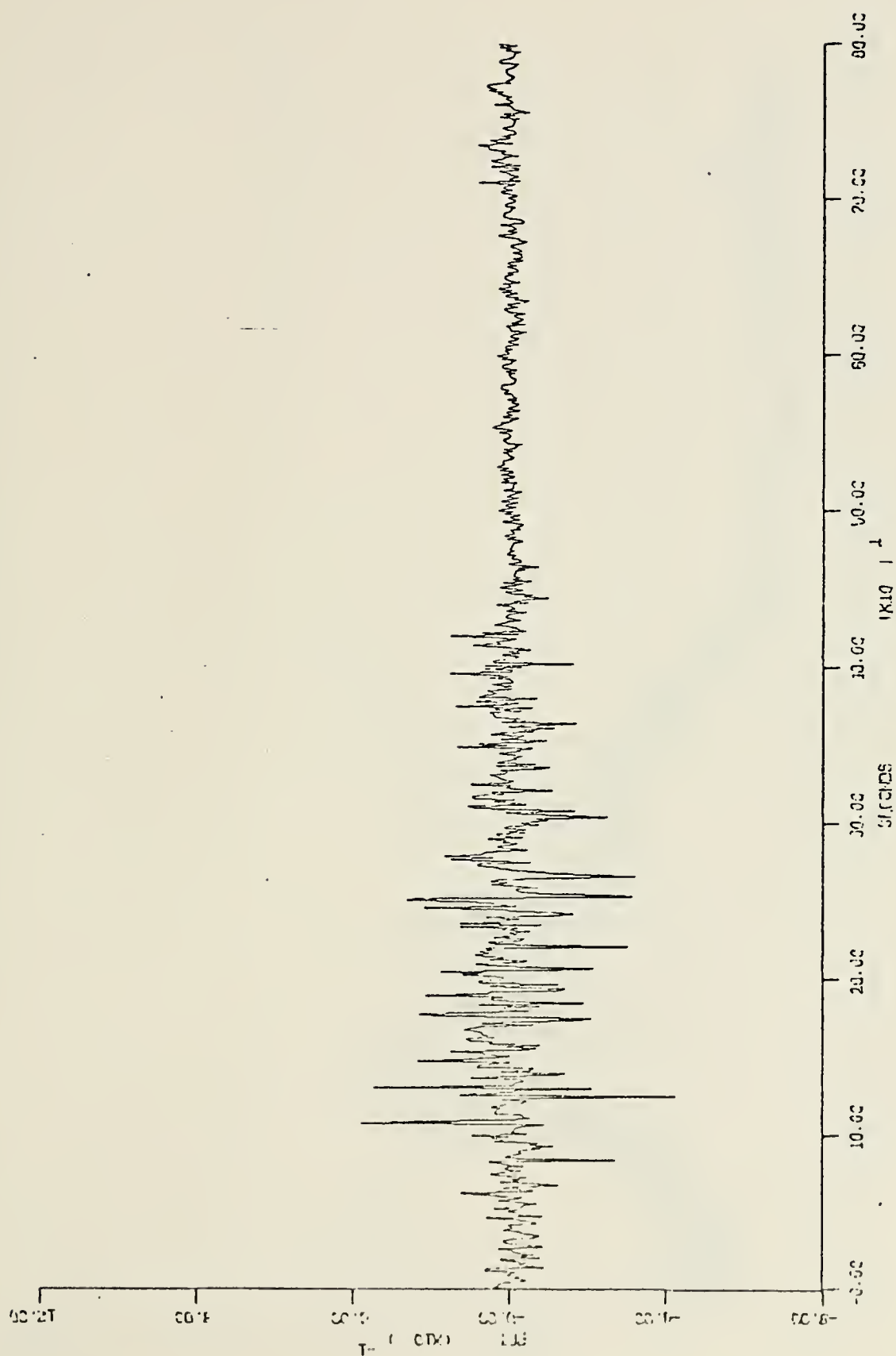


Figure 27. - Time plot of salinity - Run 12 (800 seconds).



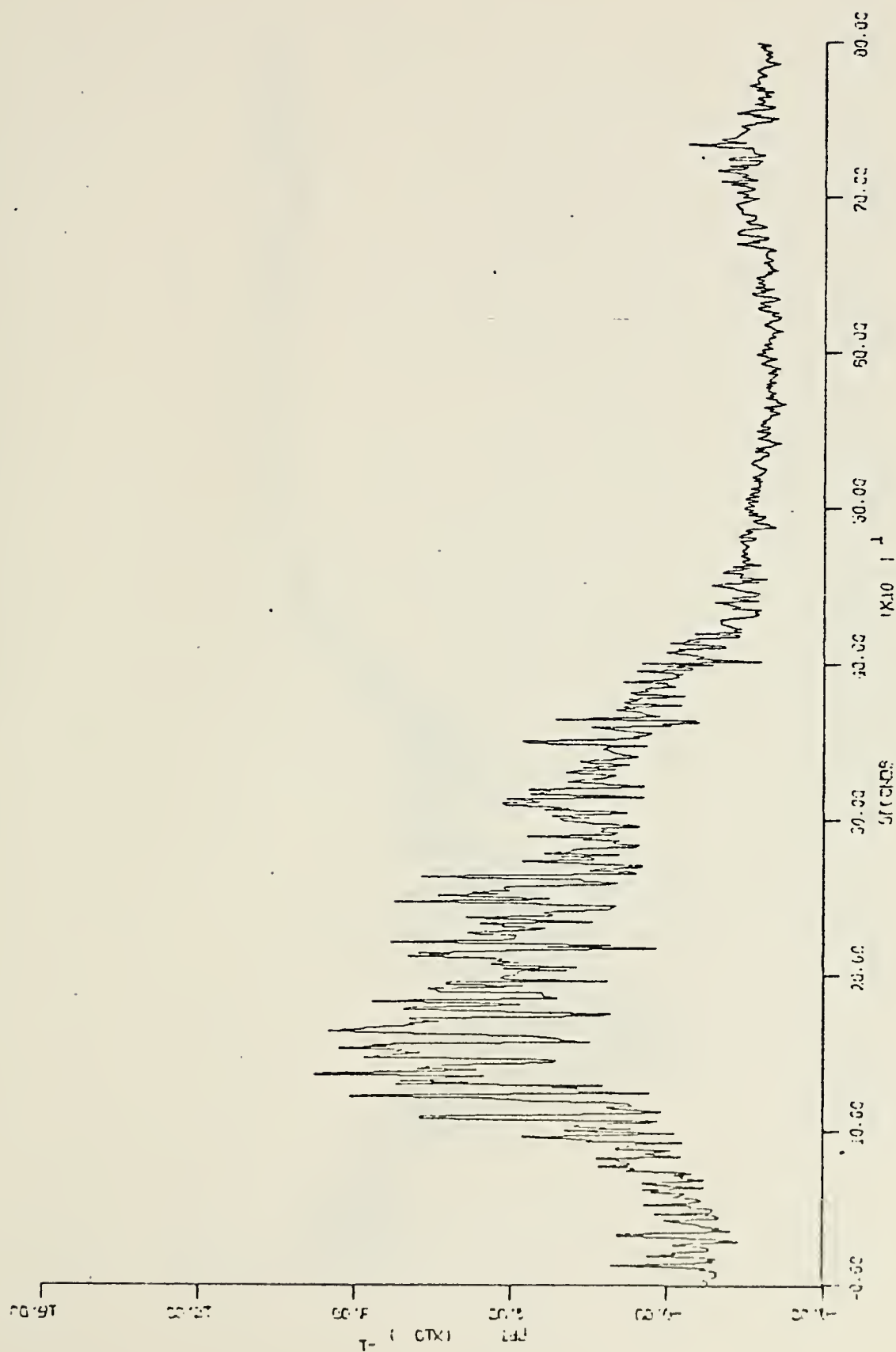


Figure 28. - Time plot of conductivity in equivalent salinity -- Run 12 (800 seconds).





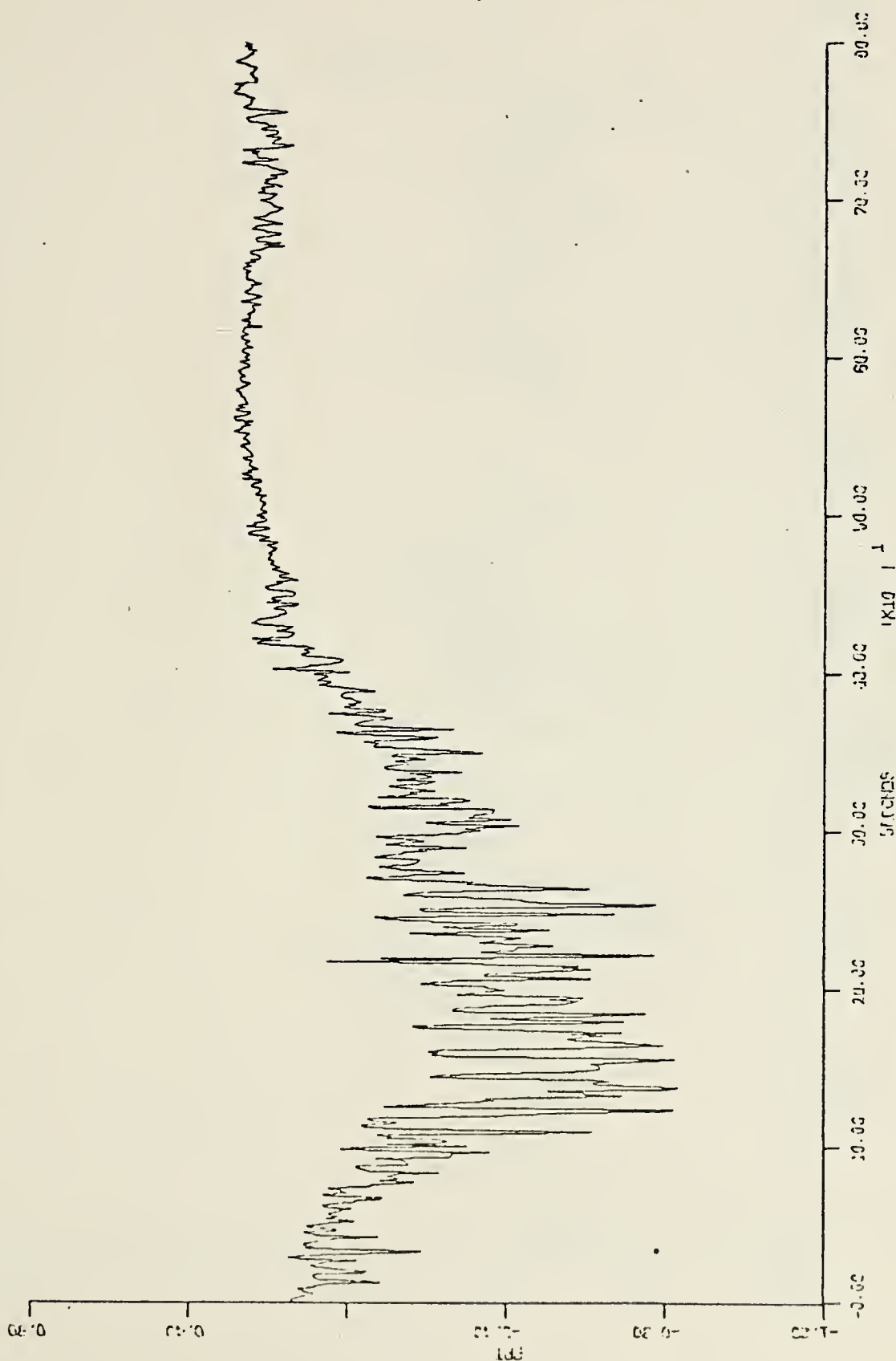


Figure 29. - Time plot of temperature in equivalent salinity - Run 12 (800 seconds).



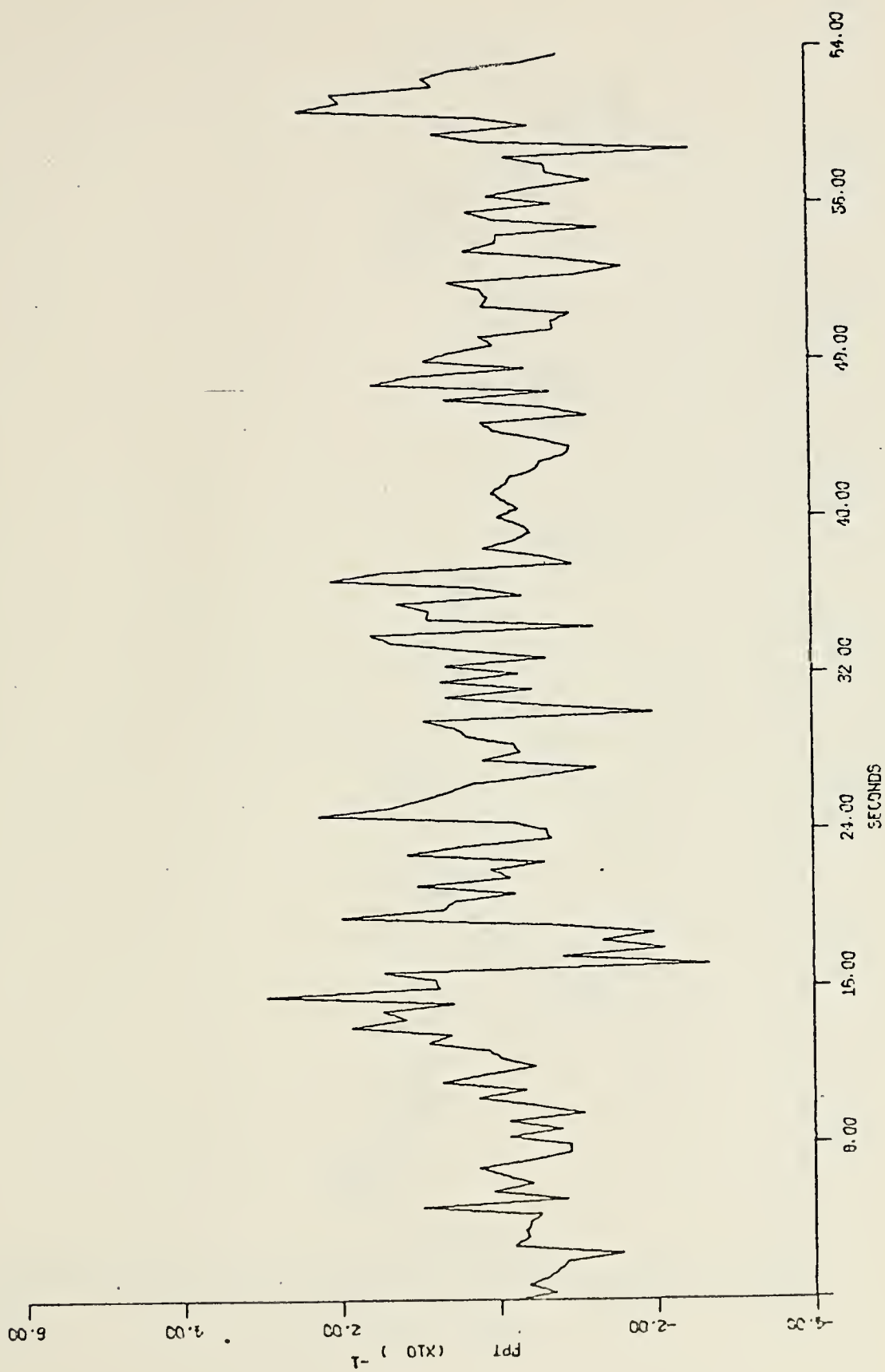


Figure 30. Time plot of salinity - Run 12 (64 seconds).



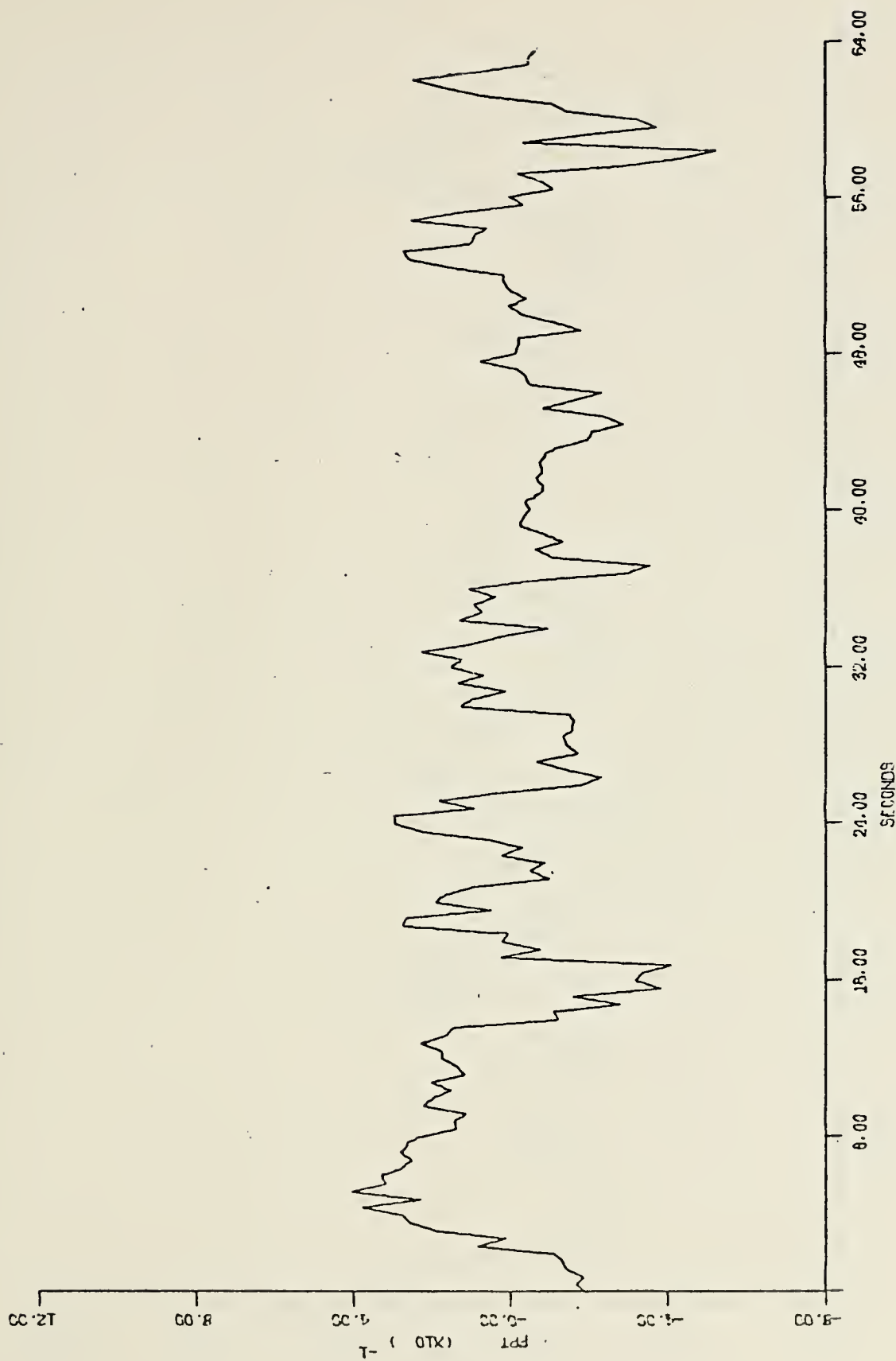


Figure 31. Time plot of conductivity - Run 12 (64 seconds).



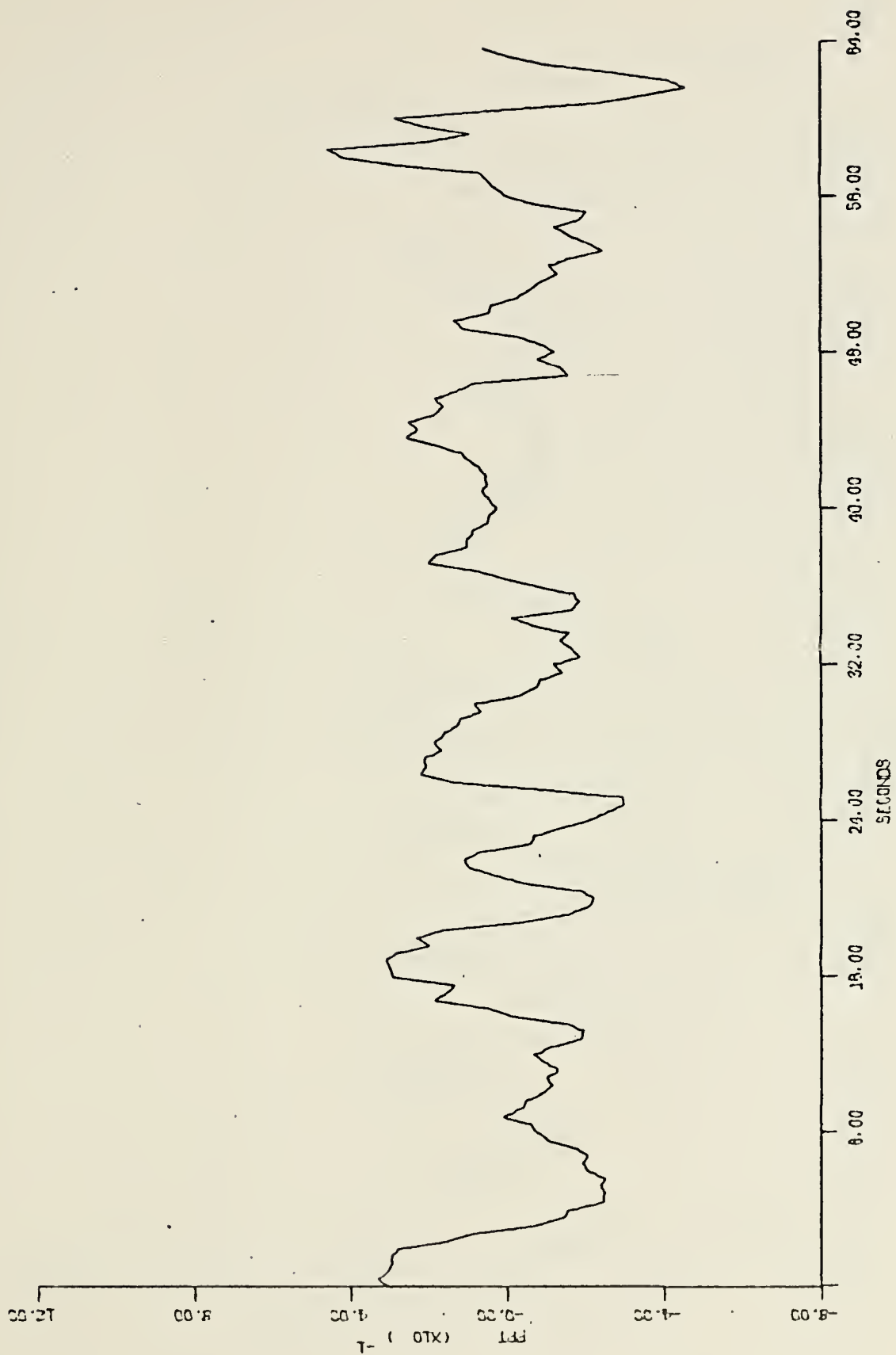


Figure 32. Time plot of temperature - Run 12 (64 seconds).





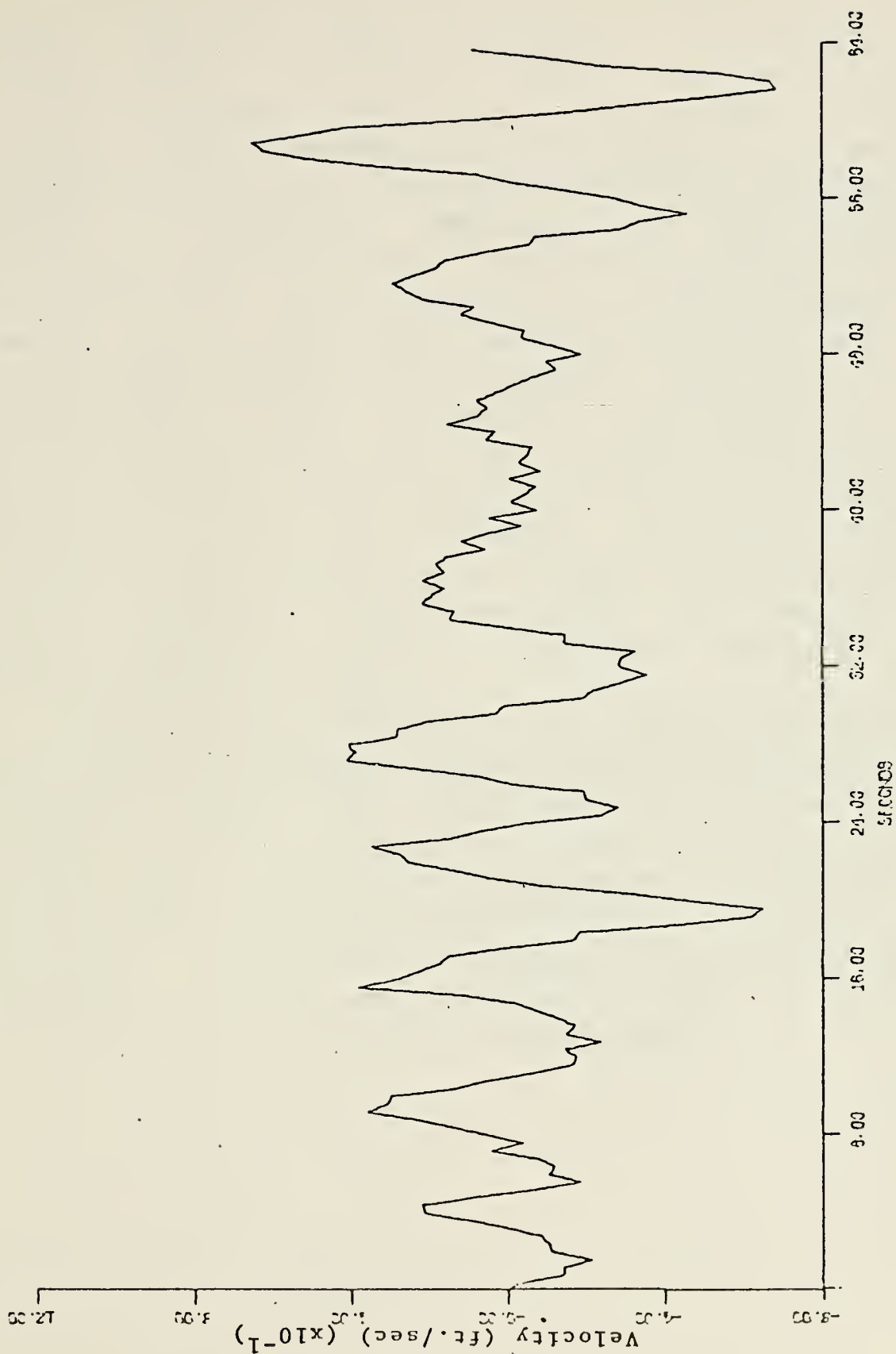


Figure 33. - Time plot of vertical fluid particle velocity - Run 12 (64 seconds).



From analysis of data and from bathythermograph data taken during the runs, an idea of the structure of temperature and salinity may be implied. Temperature was almost isothermal down to the thermocline. In the thermocline there existed a layered microstructure in which temperature had sharp step decreases between the layers. Below the thermocline temperature is again nearly isothermal. Salinity did not exhibit the large changes seen in temperature. Instead it tended to be well mixed over the entire water column. There was no large salinity gradient corresponding to that of temperature which was the thermocline. Both temperature and salinity had inhomogenities existing on the microscale. However, temperature was dominated by the large scale changes while salinity had only the microscale variations. Hence temperature was observed to be much more responsive to wave induced motion while salinity responded only somewhat to wave motion, but largely to turbulent motion of the microscale inhomogenities.

From the above discussion two conclusions are drawn concerning the mechanisms responsible for the variances of computed salinity. The first is time delay caused by seperation of the conductivity probe and thermistor. The longer time constant of the thermistor may also contribute to the delay. The other mechanism is actual variations of salinity. Because of the complex coupling mechanisms involved, the real variations of salinity cannot be readily separated from the time delay induced phenomena.



## VII. CONCLUSIONS

The conductivity instrument functioned very well in the ocean environment. Analysis of the data obtained from this instrument proved reasonable in comparison with temperature data. Temperature variations strongly influence conductivity at lower frequencies (less than .5 Hz). At higher frequencies, salinity microstructure is more dominant in its effects on conductivity.

The computation of salinity from conductivity and temperature provided mixed results. Salinity did not change much from the mean when compared with conductivity and temperature changes during internal wave passage. This implies that the water was, on the average, well mixed with respect to salinity but not temperature. The fluctuations of salinity about the mean can be accounted for by conductivity and temperature instrument mismatch and separation and by actual salinity microscale variations.

From the analysis of results, the computed salinity could be used in the computation of sound velocity. Even though the variance of salinity would be reduced with the elimination of the mismatch caused spikes, the presently determined variances are so small that they do not significantly contribute to the variance of sound velocity.

For future studies of salinity microstructure, it is suggested that it would be better to place a thermistor with a smaller time constant, directly on the conductivity probe in the vicinity of the orifice. This will greatly reduce the time constant mismatch encountered in this project. Data for computation of salinity will then not have the spurious variations. Instead, a very accurate representation of salinity microstructure may be obtained.



## BIBLIOGRAPHY

1. Batchelor, G.K., "Small Scale Variations of Convected Quantities Like Temperature in a Turbulent Fluid (Part 1)," J. Fluid Mechanics, v. 5, p. 113-133, 1959.
2. Bordy, W.B., Spectral Measurements of Water Particle Velocities Under Waves, M.S. Thesis, Naval Postgraduate School, Monterey, California, 1972.
3. Bub, F.L., Surf Zone Wave Kinematics, M.S. Thesis, Naval Postgraduate School, Monterey, California, 1974.
4. Davidson, K.L., An Investigation of the Influence of Water Waves on the Adjacent Airflow, Ph.D. Dissertation, University of Michigan, 1970.
5. Diamond, J.E., "An Inductive Conductivity Meter for Monitoring the Salinity of Dialysis Water," IEEE Transactions on Bio-Medical Engineering, v. BME-17(2), p. 109-117, 1970.
6. Duchock, C.J., Jr., The Measurement and Correlation of Sound Velocity and Temperature Fluctuations Near the Sea Surface, M.S. Thesis, Naval Postgraduate School, Monterey, California, 1972.
7. Frigge, W.J., Shallow Water Experiment Utilizing the STD Model 9006 at a Fixed Point, M.S. Thesis, Naval Postgraduate School, Monterey, California, 1973.
8. Gossner, J., Comparison of Measured and Calculated Sound Velocity Near the Sea Surface, M.S. Thesis, Naval Postgraduate School, Monterey, California, 1973.





9. Grant, H.L., Huges, B.A., Vogel, W.M. and Molliet, a., "The Spectrum of Temperature Fluctuations in Turbulent Flow," J. Fluid Mechanics, v. 34, p. 423-442, 1968.
10. Gregg, M.C. and Cox, C.S., "Measurements of Oceanic Microstructure of Temperature and Electrical Conductivity," Deep-Sea Research, v. 18(9), p. 925-934, 1971.
11. Hagen, J.B., Acoustic Fluctuations from Shallow Water Thermomicrostructure, M.S. Thesis, Naval Postgraduate School, Monterey, California, 1974.
12. Krapohl, R.F., Wave Induced Water Particle Motion Measurements, M.S. Thesis, Naval Postgraduate School, Monterey, California, 1972.
13. Neshyba, S., Neal, V.T. and Denner, W.W., "Spectra of Internal Waves: In Situ Measurements in a Multilayered Structure," J. Physical Oceanography, v. 2(1), p. 91-95, 1972.
14. Osborn, T.R. and Cox, C.S., "Oceanic Fine Structure," Geophysical Fluid Dynamics, v. 3, p. 321-345, 1972.
15. Seymour, H.A., Statistical Relations Between Salinity, Temperature and Speed of Sound in the Upper Ocean, M.S. Thesis, Naval Postgraduate School, Monterey, California, 1972.
16. Stommel, H. and Federov, K.N., "Small Scale Structure in Temperature and Salinity Near Timor and Mindanao," Tellus, v. 19, p. 306-325, 1968.



17. Thompson Ramo Wooldridge Report No. 8609-0100-RU-000,  
Measurement of Temperature, Salinity, and Velocity of  
Water Through Electrolytic Conductivity Measurements,  
by L.L. Higgins, 1962.
18. Whittemore, M.A.N., Small Scale Temperature Fluctuations  
Near the Sea Surface, M.S. Thesis, Naval Postgraduate  
School, Monterey, California, 1973.



# INITIAL DISTRIBUTION LIST

- |    |   |   |
|----|---|---|
| 1. | Department of Oceanography, Code 58<br>Naval Postgraduate School<br>Monterey, California 93940                                | 3 |
| 2. | Oceanographer of the Navy<br>Hoffman Building No. 2<br>200 Stovall<br>Alexandria, Virginia 22332                              | 1 |
| 3. | Office of Naval Research<br>Code 480<br>Alexandria, Virginia 22217  | 1 |
| 4. | Dr. Robert E. Stevenson<br>Scientific Liason Office, ONR<br>Scripps Institution of Oceanography<br>La Jolla, California 92037 | 1 |
| 5. | SIO Library<br>University of California, San Diego<br>P.O.Box 2367<br>La Jolla, California 92037                              | 1 |
| 6. | Library, Code 3330<br>Naval Oceanographic Office<br>Washington, DC 20373  | 1 |
| 7. | Department of Oceanography Library<br>Washington State University<br>Seattle, Washington 98105                                | 1 |



8. Department of Oceanography Library 1  
Oregon State University  
Corvallis, Oregon 97331
9. Commanding Officer 1  
Fleet Numerical Weather Central  
Monterey, California 93940
10. Commanding Officer 1  
Environmental Prediction Research Facility  
Monterey, California 93940
11. Department of the Navy 1  
Commander Oceanographic System Pacific  
Box 1390  
FPO San Francisco 96610
12. Defence Documentation Center 2  
Cameron Station  
Alexandria, Virginia 22314
13. Library (Code 0212) 2  
Naval Postgraduate School  
Monterey, California 93940
14. Dr. Noel E Boston, Code 58 (thesis advisor) 3  
Department of Oceanography  
Naval Postgraduate School  
Monterey, California 93940
15. Dr. Edward B. Thornton, Code 58 1  
Department of Oceanography  
Naval Postgraduate School  
Monterey, California 93940





16. Dr. Robert G. Paquette, Code 58 1  
Department of Oceanography  
Naval Postgraduate School  
Monterey, California 93940
17. LT Leonard K Kane II (USN) 1  
USS DACE (SSN 607)  
FPO New York, N. Y. 09501
18. LT James B. Hagen (USN) 1  
USS BENJAMIN FRANKLIN (SSBN 640) Gold  
FPO New York, N. Y. 09501
19. Dr. Warren W. Denner 1  
Director  
Naval Arctic Research Laboratory  
Barrow, Alaska 99723



Thesis  
K1416 Kane  
c.1

155607

Measurement and analysis of temporal variations of salinity in shallow water.

Thesis  
K1416 Kane  
c.1

155607

Measurement and analysis of temporal variations of salinity in shallow water.

thesK1416

Measurement and analysis of temporal var



3 2768 002 11404 3

DUDLEY KNOX LIBRARY